Effect of Zr and Ti on the phase evolution of silicon oxycarbide ceramics

Soumya Prakash Sahoo

Department of Ceramic Engineering
National Institute of Technology Rourkela

Effect of Zr and Ti on the phase evolution of silicon oxycarbide ceramics

Thesis submitted in partial fulfillment

of the requirements of the degree of

Dual Degree

in

Ceramic Engineering

by

Soumya Prakash Sahoo

(Roll Number: 711CR1158)

based on research carried out

under the supervision of

Prof. Shantanu Kumar Behera

May, 2016

Department of Ceramic Engineering

National Institute of Technology Rourkela

Department of Ceramic Engineering
National Institute of Technology Rourkela

Prof. Shantanu Kumar Behera
Assistant Professor

May 31, 2016

Supervisor's Certificate

This is to certify that the work presented in the dissertation entitled *Effect of Zr and Ti on the phase evolution of silicon oxycarbide ceramics* submitted by *Soumya Prakash Sahoo*, Roll Number 711CR1158, is a record of original research carried out by him under my supervision and guidance in partial fulfillment of the requirements of the degree of *Dual Degree* in *Department of Ceramic Engineering*. Neither this thesis nor any part of it has been submitted earlier for any degree or diploma to any institute or university in India or abroad.

_____
Shantanu Kumar Behera

Acknowledgment

I am indebted to a number of personalities who have helped me accomplishing this report. I apologize if I inadvertently missed someone for not being diligent enough. On the foremost part, thank you God for easing the journey in this endeavor.

I wish to express my sincere gratitude to my advisor Prof. Shantanu Kumar Behera for his supervision, guidance, encouragement and support during the course of this thesis and in the experimental study. His appreciation of however little achievements, pulling me back into the nitty-gritty of the study whenever I diverted, the genius of him for always finding an alternate route when another closed, and the freedom he provided to inculcate a research mind set in a novice, are the sole reasons for the completion of this thesis. A special mention to Prof. Santanu Bhattacharya for providing me with the books that even Google could not provide. Although I could not gain any weight, how much he wished me to, but I sure did gain a remarkable amount of knowledge from the little discussions that we had on the topic.

My heartfelt thanks to Abhisek *bhai* for his true Indian *jugaadu* skills. Be it a mere tweezer or a rare copper grid—you want it, confide it in him and *voila!* There you have it! Jairao *bhai* for helping me learn the nuances of research, Biswajeet *bhai* for the tech (read torrent) support, and Pranati *nani*, Ipsita and Pallavi *nani* for their invaluable suggestions and comments during the seemingly unending hours spent in the lab.

I must thank all my professors for putting up with my childish doubts and not losing their minds all these years and shaping a kid to not-a-kid-anymore. Arvind Sir, Bapi *da*, Sukanta *da* and all other staff members of the Ceramic Engineering Department are worth a special mention for hastening the work when it seemed to stall. My friends, especially the *Vees* and my dual degree mates, for their unflinching support and for the constant reminder of the biometric attendance.

Last but not the least, my parents and my kid brother for the unconditional love and constant encouragement, forgiving me for not being able to visit home during vacations, and for the constant motivation during my lows, thank you. Your faith in me acted as my fuel.

Thank you for being there. Thank you, everyone.

May 31, 2016
NIT Rourkela

Soumya Prakash Sahoo
Roll Number: 711CR1158

Abstract

Si based polymer-derived ceramics (PDCs) have been gaining attention due to their exceptional functional and ultrahigh temperature properties. With excellent creep resistance even at temperatures far beyond 1000°C and resistance in oxidative as well as corrosive environment, PDCs have emerged as potential materials in the fabrication of thermo-structural composites. Among the many PDCs, including SiC, SiCN, SiOC, and SiCBN, SiOC can be fabricated from commercially available polysiloxanes or polysilsesquioxanes. However, silicon oxycarbide based PDCs exhibit relatively limited oxidation resistance and high temperature performance compared to their nitride/carbonitride counterparts. In addition, these ceramics should be compatible with carbide based substrates and oxide based top coats for thermal protection systems.

Preliminary work has indicated that incorporation of transition metals into the Si-O-C system exhibits interesting crystallization, oxidation, and thermal stability. This work demonstrates the behaviour of Zr and Ti, introduced as a molecular source, in the phase evolution, crystallization, and oxidation resistance of the polymer-derived SiMOC (where M = Zr, Ti) ceramics. A commercially available preceramic polymer was doped with 5−20mol% of the dopant metal ion (through alkoxide source), and cross-linked. Inert atmosphere pyrolysis of thus produced powders yielded black coloured SiMOC ceramics. X-ray diffraction (XRD) analysis was employed to observe the phase evolution. It was revealed that Ti ions crystallized into carbide phase at temperatures as low as 1200°C, while the Zr ions phase separated into t-ZrO_2 whose crystallite size was calculated from the X-ray diffractograms using Scherrer formula. In both of the systems the phase separation of SiO_2 was observed at temperatures beyond 1300°C. The crystallites of the formed SiC, TiC and ZrO_2 were further analyzed by transmission electron microscopy (TEM). Since carbide phase was formed in the Ti-doped ceramic, thermogravimetric (TG) tests were performed to study the mass loss of the ceramic in both inert and oxidative atmospheres. The chemical nature of SiTiOC ceramic was investigated by Fourier-transform infrared (FTIR) spectroscopy. To support a hypothesis on the placement of the dopant atoms in the SiOC structure, *ab initio* calculations based on simple bond-counting method were also performed.

***Keywords*: *Polymer-derived ceramics*; *phase evolution*; *silicon oxycarbide*; *Ti-doped SiOC*; *Zr-doped SiOC*; *oxidation resistance*.**

Contents

List of Figures

List of Tables

Chapter 1

Introduction

Several ceramic fabrication processes are used to produce commercial products that vary in shape, size, composition, complexity, and cost. The fabrication of a ceramic normally includes some ceramic materials, some liquids and some special additives called processing aids. Several operations are employed to manufacture the product from a batch containing ceramic materials and processing additives into a near defect-free finished product. These operations need to be carefully controlled. A scheme for the several types of ceramic-forming techniques is presented in Figure 1.1 and the respective products formed are tabulated in Table 1.1.

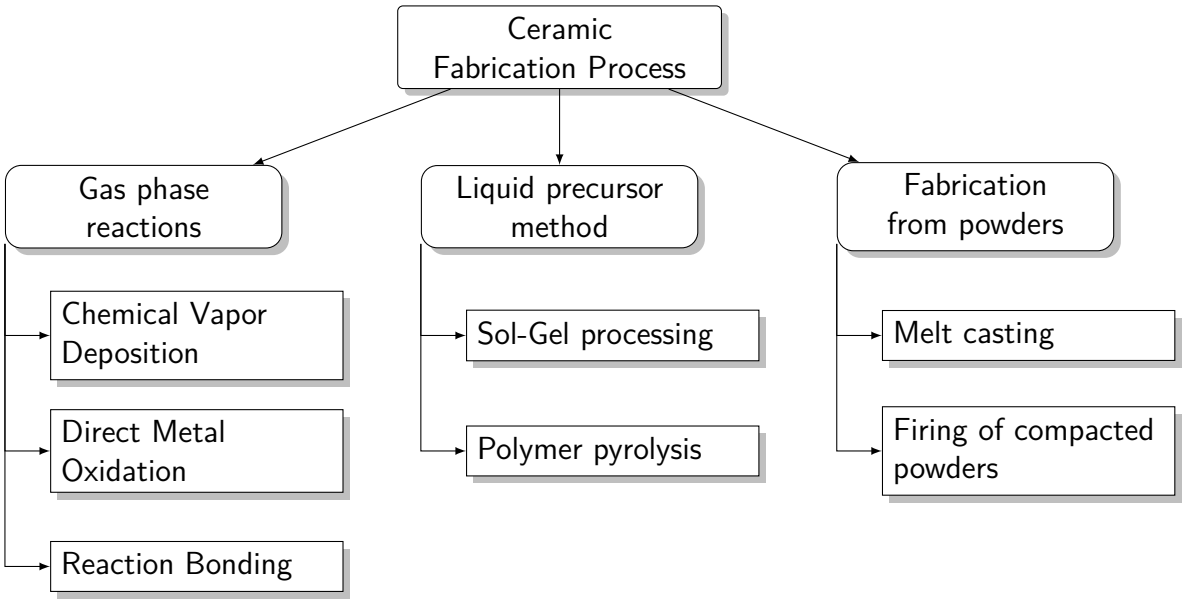

Figure 1.1: Overview of some common fabrication processes

1.1 Polymer derived ceramics

Polymer derived ceramics (PDCs) are a novel class of complex nanostructured ceramics, which can be produced in an inert or reactive atmosphere upon cross-linking and controlled pyrolysis of suitable polymers. These additive-free ceramics cannot be obtained by any

Table 1.1: Common ceramic fabrication techniques [1]

Precursor	Method	Product
Gases	Chemical vapor deposition	Films, monoliths
Gas-liquid	Direct metal oxidation	Monoliths
Gas-solid	Reaction bonding	Monoliths
Liquid-solid	Reaction bonding	Monoliths
Liquids	Sol-gel process	Films, fibers
	Polymer pyrolysis	Fibers, films
Solids (powders)	Melt casting	Monoliths
	Sintering of powders	Monoliths, films

other techniques [2]. The classes of PDCs are divided into binary systems (SiC, Si_3N_4 and BN), ternary systems (SiOC, SiCN and BCN) and quaternary systems (SiCNO, SiBCN and SiBCO). Pentanary systems have also emerged in recent years [3, 4].

The PDCs have been gaining attention for their outstanding high temperature thermal stability, stability with respect to crystallization as well as resistance in oxidative and corrosive environments. The microstructure and phase composition of the PDCs strongly influence their properties. Hence, chemistry and the molecular structure of the preceramic polymer form important parameters for the modification of the properties of PDCs.

1.1.1 Polymeric precursor

Conventional organic polymers like polyethylene contain a chain of carbon atoms. Preceramic polymers are different than the conventional ones since the chain backbone in preceramic polymers contains Si-backbone with other elements (e.g., B, and N) in the chain other than carbon or in addition to carbon [1]. Suitable precursors like organosilicon preceramic polymers are only used for the synthesis of ternary ceramics such as SiOC since carbon has a low solubility in SiO_2. Thus for incorporation of relatively large amounts of free carbon into the ceramic structure, these materials are synthesized by pyrolysis of the preceramic polymers in an inert gas atmosphere [5–9]. An oversimplified molecular stucture of organosilicon polymer has been represented in Figure 1.2 where R^1 and R^2 are the functional groups and variation in (X) generates different classes of Si-based polymers. Some of these classes of polymers are shown in Table 1.2. As compared to the low-carbon containing PDCs, these carbon-rich analogues have shown a higher ceramic yield along with a higher resistance against crystallization [5, 9].

Figure 1.2: An oversimplified molecular stucture of organosilicon preceramic polymer

Si-based polymer	(X)
Poly(organosilane)	Si
Poly(organocarbosilane)	CH_2
Poly(organosiloxane)	O
Poly(organosilazane)	NH
Poly(organosilylcarbodiimides)	N=C=N

Table 1.2: Different classes of Si-based polymers on variation of group (X)

The composition, amount of phases along with the phase distribution and the microstructure of the final ceramic are influenced by the type of preceramic polymer and its molecular structure. These polymeric precursors need to have high molecular weight to avoid the volatilization of low molecular components. Presence of functional groups in the polymeric chains would enable the curing and cross-linking. Moreover, appropriate rheological properties and solubility determine the shaping process. These properties of the preceramic polymers render them effective for thermal decomposition [2].

Polysilsesquioxanes, the class of preceramic polymers used in the present work, have a general molecular structure of $-[RSi-O_{1.5}]_n-$. Poly(methyl phenyl)silsesquioxane (PMPS) is a powdered silicon resin which has excellent heat stability and high solubility in organic solvents. With an average molecular weight of 2100 g/mol, the general formula of the PMPS polymer is $[Ph_{0.62}Me_{0.31}R_{0.07}SiO_{1.5}]_n$ with $n > 20$ where Ph is the phenyl group, Me is the methyl group, and R= $-OC_2H_5$ and $-OH$ [10]. These hydroxy and ethoxy groups are responsible for the cross-linking in the ceramic.

1.1.2 Polymer pyrolysis process

The pyrolytic decomposition of the organometallic polymer to produce ceramics is referred as polymer pyrolysis. These organometallic polymers are the preceramic polymers. This route is quite related to the sol−gel process where the synthesis of a metal-organic polymeric gel takes place and is converted to an oxide. Conventional fabrication techniques involve sintering of the ceramics where the sintering temperature can range up to 2500°C. The basic advantage of the polymer pyrolysis process is that it allows the fabrication of near net shaped ceramics at lower temperatures of 500−1500°C compared to the conventional powder sintering route.

The conversion from polymer-to-ceramic takes place in two steps:

I Cross-linking of the polymers at lower temperatures of 100−400°C

II Pyrolysis at temperatures up to 1000−1500°C resulting in ceramization of the polymer

Cross-linking in the polymer takes place due to the hydroxy or ethoxy group present in the structure. Condensation of the Si−OH units and subsequent loss of water as well as the

hydrolysis of the alkoxy groups result in Si−O−Si bond. The schematic of the condensation and hydrolysis reactions has been shown in Figure 1.3. Pyrolysis of the polymer results in an amorphous ceramic which upon futher increase in temperature yields nanocrystalline inorganic materials.

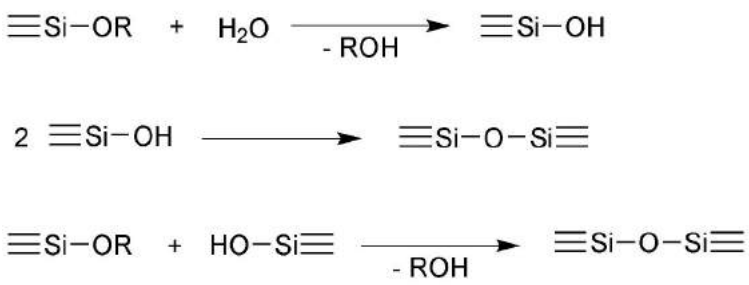

Figure 1.3: The condensation and hydrolysis reactions that take place during the cross-linking of polysiloxanes/sesquioxanes polymer

1.2 Application of PDCs

Due to the possibility of various designs in the molecular architechture of the preceramic polymer, fabrication of multifunctional PDCs with tailored properties is achievable. The fields in which PDCs have found an application are:

- High temperature resistant materials (energy materials, automotive, aerospace, etc.)
- Chemical engineering (catalyst support, food and biotech, etc.)
- Functional materials, including sensors, and anodes for Li-ion batteries

PDCs are suitable candidates in the field of energy and environment systems, defence, transport, biomedical components and micro- and nano-electromechanical systems (MEMS/NEMS) [2, 11, 12]. SiOC and SiCN PDCs have been shown to be potential candidates as force and pressure sensors in harsh environments [13, 14] and in electrical storage and mobile applications [2, 12]. PDC based based Li-ion battery anodes have been found to be advantageous than the graphite-based anodes [15, 16]. PDCs, with their high strength, stability in oxidative and corrosive environments, creep and thermal shock resistance, have been proved to be promising materials for use in extreme conditions in such applications.

1.3 Outline of the present work

In this present work on the effect of Zr and Ti on the phase evolution of silicon oxycarbide ceramics, Chapter 1 provides a general introduction on the topic in hand. The class of

polymer derived ceramics and the method of fabrication have been briefed in this section. The previous works done in this area have been outlined in Chapter 2. The aspects regarding the modification of the preceramic polymers have mainly been focussed. Chapter 3 presents the experimentations carried out to study the effect of the transition metals on the SiOC ceramics. Preliminary investigations on the thermal behavior and the phase evolution in the preceramic polymer used in this study has been presented in Chapter 4. The effect of Zr and Ti on the silicon oxycarbide ceramics form the vitals of this chapter. The chapter ends with the *ab initio* calculations to support the hypothesis regarding the placement of the dopant atom in the polymer network. Finally, the conclusions drawn out from the study have been outlined in Chapter 5.

Chapter 2

Literature Review

In the past two decades, almost 1500 papers have been published which have been denoted as 'Si-based polymer-derived ceramics (PDCs)' (Figure 2.1). PDCs have become the current area of research due to their excellent properties at ultrahigh temperatures with respect to decomposition and crystallization process.

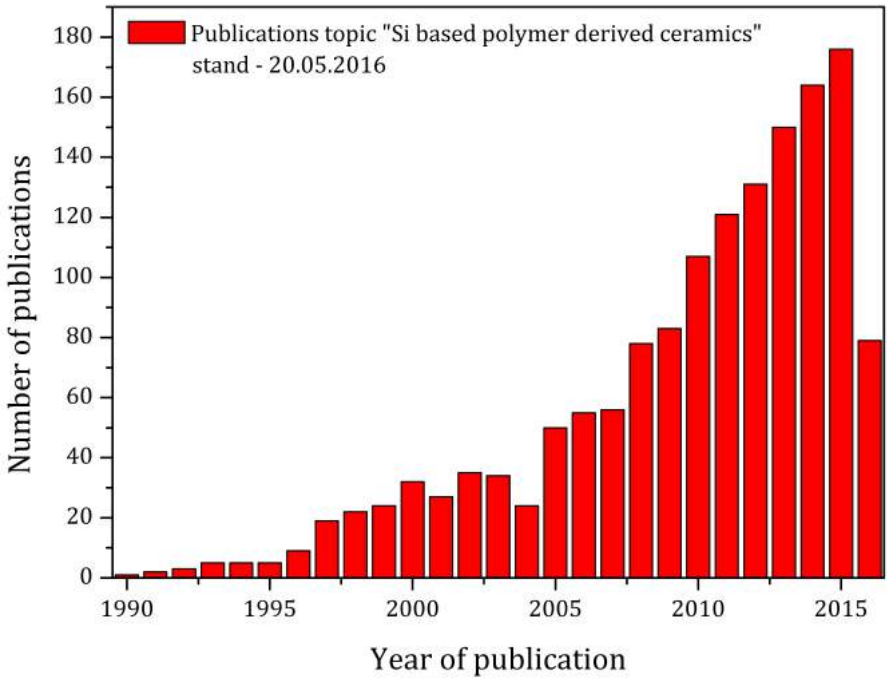

Figure 2.1: Number of publications resulting from a search with the keyword ''Si-based polymer-derived ceramics'', from 1990 up to now.

PDCs are known to be prepared by the solid-state thermolysis of preceramic polymers [2, 17, 18]. Upon the pyrolysis of organosilicon polymers, these Si-based PDCs can be directly synthesized [2]. Fritz and Raabe [19] built the premise of this area where they produced organosilicon compounds via the thermal decomposition of a cyclic class silicon-hydrocarbon compounds. Later, works of Ainger and Herbert [20], Chantrell and Popper [21] furthered the research on this area where they produced non-oxide ceramics deriving them from molecular precursors. It was Yajima *et al* [22, 23] who pioneered on the

production of SiC fibers by the thermolysis of polyorganocarbosilanes. Since the work of Yajima, several significant advances in the field of synthesis and processing of PDCs have been achieved [2, 17, 18].

Under a controlled atmosphere and proper curing and thermolysis processes, the preceramic polymers undergo a polymer-to-ceramic conversion and produce the ceramics, thus known as polymer derived ceramics. The respective ceramic that some polymeric precursors yield upon pyrolysis have been tabulated in Table 2.1, along with the corresponding works done in the field. It has been reported that the ternary based PDCs like silicon oxycarbide (SiOC) and silicon carbonitride (SiCN) ceramics have shown excellent thermomechanical properties [24–26], resistance in oxidative and corrosive environments [27, 28] as well as ultrahigh temperature properties [29, 30].

Preceramic polymers	Yielded ceramic	References
Polysiloxane	C, SiO_2, SiC, SiOC	[31–33]
Polycarbosilane	SiC, SiOC	[34–37]
Polysilazane	Si_3N_4, SiCN	[38–44]
Polyborosilazane	SiBCN	[45, 46]

Table 2.1: Final ceramic product obtained upon controlled atmosphere pyrolysis of some polymeric precursors

The structures of these polymer derived ceramics have been modified by addition of fillers which was the scope of research in the last decade to produce crack free bulk ceramic components [38, 47, 48, 50, 51]. In this technique, the polymer is partially filled with inert or active fillers which are basically powder particles. These particles compensate for the shrinkage produced due to the outgassing of the organic material during pyrolysis of the polymer. Thus, incorporation of these fillers permits the fabrication of crack free bulk ceramics. This technique has been termed as active filler controlled polymer pyrolysis process (AFCOP) [39, 52, 53].

The properties of the preceramic polymers can be directly influenced by its stucture and synthesis [54]. Thus, apart from the incorporation of fillers in the polymer precursor, with certain modification in the chemical structure of the polymer itself can lead to quarternary ceramics with improved properties than their ternary counterparts. This advantage has been seen in boron modified SiOC ceramics (SiBOC) where the SiC in the SiBOC ceramics crystallized at a lower temperature than the pure SiOC [55–58].

Although prior works [49, 59, 60] have been carried out where Ti acts as an active filler in the preceramic polymer, few works [61] have been done where SiOC has been chemically modified with Ti as a molecular source. Hybrid polydimethylsiloxane-titania nanocomposites have been synthesized by sol-gel process. The pyrolytic transformation

of polydimethylsiloxane/ titania hybrid xerogels was studied by varying the titania content. For the completion of the polymer-to-ceramic conversion, higher temperatures were required upon decreasing the TiO_2 content. XRD spectra revealed that as the carbon content decreased in the ceramic between the temperature regime of $1000-1600°C$, the SiOC phase underwent a continuous structural evolution thereby forming pure SiO_2 at 1600°C [61].

The decomposition and crystallization at high temperature of Zr and Hf doped SiOC has been investigated by various research groups [62–65]. Polysilsesquioxane was modified by addition of metal alkoxides and was cross-linked followed by pyrolysis at 1100°C to obtain the ceramics. The crystallization and microstructural evolution had unique behavior in different temperature regimes. Below 800°C the material remained amorphous with a single phase of SiMOC (M=Zr, Hf). The HRTEM/EELS data showed the single phasic amorphous nature of SiHfOC [63]. Phase separation in the amorphous ceramic started at temperatures of $800-1000°C$. It phase separated into metal oxide nanoparticles. HRTEM analysis revealed the phase separation of HfO_2 in this temperature regime which showed an amorphous SiOC matrix with dispersed amorphous hafnia nanoparticles [63]. In the temperature regime of $1000-1400°C$, the amorphous metal oxide crystallized into t-MO_2 along with phase separation of the SiOC matrix. The SiOC matrix fully phase separated into silica, β-SiC nanoparticles and segregated carbon. The particle size of the t-ZrO_2 and t-HfO_2 precipitates were in the range of $2-5$ nm. Moreover, these nano crystals were well dispersed in the SiOC matrix. Thus, due to the small size and dispersion of the t-MO_2 precipitates, phase transformations fron tetragonal to monoclinic did not occur [62, 63]. Upon further increase in the pyrolysis temperature beyond 1400°C, crystalline metal silicate nanoparticles of size $20-50$ nm were formed. These nanoparticles were the direct effect of solid state reactions between SiO_2 and the MO_2 phase [62, 63]. Similar behavior was also found in SiAlOC [66], SiMnOC [67] and SiLuOC [67] ceramics.

Like the silicon oxycarbide system, modifications in the silicon carbonitride system have also been investigated. The incorporation of boron into SiCN to form a a quarternary system of SiBCN has shown to increase the crystallization resistance and the thermal stability of the ceramic, intensely [29]. Several kinetic [68] and thermodynamic [69] studies have been performed on SiBCN system to investigate the reason of the dramatic increase in thermal stability and this stability has been attributed to kinetic reasons [70, 71]. It has been reported that with increase in boron content, thermodynamic stability decreases, thus addition of boron for the crystallization of Si_3N_4 is considered to be entirely a kinetic effect [72].

Incorporation of different metals like Al [25, 28], Ti [73], Y [74, 75], Zr [76, 77] anf Hf [3, 4, 54, 78] in the SiCNO ceramics to form a multinary system of SiMCNO (where M is the metal ion) have also been reported. The polysilazanes have been modified chemically with respective metal alkoxides and are subsequently pyrolyzed to prepare amorphous SiMCNO ceramics. At higher temperatures, these ceramics phase separate to form amorphous metal oxides which remain dispersed in an amorphous SiCNO matrix. Upon further annealing at

higher temperatures, these amorphous metal oxides crystallize into nanoparticles.

Among these modified ceramics, the Hf doped system has been extensively studied. The single-phase amorphous SiHfCNO formation at 700−800°C has been supported by ^{29}Si MAS NMR studies while TEM studies showed the phase separation into amorphous HfO_2 [78]. At temperatures beyond 1300°C, nanocomposites of crystalline t-HfO_2/SiCNO are formed which subsequently crystallize into β-Si_3N_4 and β-SiC upon further increase in the temperature. It has been reported [54] that at 1600°C, the mass loss in the SiHfCNO ceramics is ∼30 wt% lower than that in pure SiCNO, therby proving the improved high-temperature resistance of SiCNO upon modification with Hf. Studies on the solid solubility of HfO_2 have also been reported [4]. Experiments have shown that the solubility extends to a Hf/Si ratio of <0.22. The study also talks about the placement of the Hf atoms in the amorphous network where it has been proposed that the Hf atom substitutes for the Si atom in the amorphous network since the bond strengths of Hf and Si with C, O and N are similar.

2.1 Summary

The prior works done in this area can be summarized into the following points:

- Polymer pyrolysis of polymeric precursors is the only technique to produce ternary and quarternary system based polymer derived ceramics.
- Addition of inert or reactive fillers into the preceramic polymer results in additional phases in the ceramic. These fillers are commonly added in powder state. They compensate for the shrinkage in the bulk ceramics during fabrication.
- Chemical modification of the preceramic polymer by addition of metal alkoxides is a novel technique to prepare quarternary ceramics. The incorporation of dopants into the polymeric precursor affects its molecular structure. It has been shown that modification in the chemical structure of the polymer itself can lead to quarternary ceramics with improved properties than their ternary counterparts.
- Metal oxides resulted from the addition of metal alkoxides into the polymeric precursor. Few works on polymers with high carbon content to be used as polymeric precursors for production of quarternary ceramics have been reported.

2.2 Objective of the work

Thus, the following objectives were drawn out for the present study, based on the prior works:

- Synthesis of SiTiOC and SiZrOC ceramics from polymer pyrolysis method using a preceramic polymer with high carbon content.

- Study the phase evolution of the hybrid ceramics where Zr or Ti are added as a molecular source.
- Perform high resolution electron microscopy to expose the morphology and structure of the synthesized hybrid ceramics.

Chapter 3

Experimental

3.1 Materials

The preceramic polymer poly(methyl phenyl)silsesquioxane (PMPS) (commercial name: SILRES® H44) was used which was obtained from Wacker Silicones, Burghausen, Germany. Titanium(IV) isopropoxide and zirconium(IV) isopropoxide were used as precursors for Ti and Zr doping in the silicon oxycarbide ceramics respectively. Titanium(IV) isopropoxide and zirconium(IV) isopropoxide were procured from Sigma-Aldrich.

3.2 Processing of doped Silicon Oxycarbide Ceramics

Preliminary investigations of PMPS powders (refer section 4.1.1) showed that the polymer has a ceramic yield of 55%. The dopant was added into the polymer system in a ratio of metal ion to silicon. The PMPS polymer was pyrolyzed in air to find out the ceramic yield, which is SiO_2. Based on the weight of SiO_2 the Si content in the PMPS polymer was calculated. Subsequently, the amount of dopant ion in the polymer was calculated for 5, 10, 15 and 20 mol% of the dopant to Si ion in the polymer.

For batch preparation, 20 ml of isopropyl alcohol (IPA) was taken in a glass beaker to which 10 g of PMPS polymer was added. The solution was stirred continuously using a glass rod until a clear solution of the polymer was obtained. In another beaker ~10 ml of isopropyl alcohol was taken and heated (for the metal ion precursor has higher solubility in hot isopropyl alcohol). The respective metal ion precursor was measured in a measuring cylinder and poured into the hot isopropanol with constant stirring. This metal precursor solution was immediately poured into the polymer solution to prevent the formation of metal hydroxides since isopropoxide readily reacts with moisture. The mix was continuously stirred in a magnetic stirrer. 50 μl (0.5 weight%) of triethanolamine (TEA) was measured in a micro-pipette and added as a cross-linking agent into the mixture and stirred vigorously.

The resulting mix was transferred into a glass petri-dish and was kept in an electric oven at 60°C for drying. Then the dried solid was scrapped off the petri-dish and was thoroughly ground with a mortar and pestle. The ground powders were transferred into

an alumina crucible and were cross-linked in a muffle furnace at 350°C for 2 hours. The cured powders were further ground to fine powders in a SPEX mill (SPEX 8000M, SPEX SamplePrep, Metuchen, NJ, USA). These powders were finally pyrolyzed in a tube furnace under an inert argon atmosphere with a maximum dwelling time of 2 hours at the peak temperature. The pyrolysis temperature varied from 900−1500°C at a ramp rate of 3°C/min from room temperature to 1000°C and 2°C/min up to the temperature above 1000°C. Figure 3.1 schematically shows the main steps in the processing of the doped SiOC ceramic.

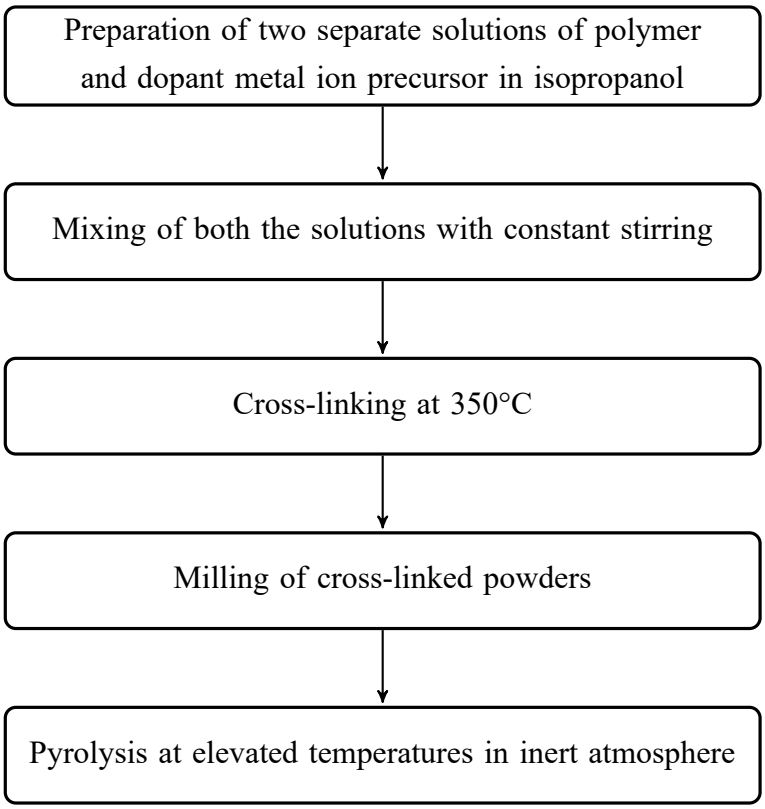

Figure 3.1: Brief overview of the batch preparation

3.3 Characterization of the as obtained Ceramics

Several analytical techniques were used to monitor the effect of dopant addition on the microstructure and thermal transformations of the obtained ceramics. The pyrolytic conversion of the preceramic polymer (PMPS) was also investigated.

3.3.1 Phase evaluation

The pyrolyzed samples of neat and doped SiOC were milled in a SPEX mill (8000M Mixer/Mill®) and the phases were identified by X-ray diffraction (XRD) technique using Rigaku Ultima IV X-ray diffractometer with CuKα radiation. The samples pyrolyzed at elevated temperatures (900−1500°C) were placed in glass sample holders and analyzed at

diffraction angles between 15−80° at 20°/min and a step size of 0.05°. The effect of pyrolysis temperature and amount of dopant was studied from the diffractograms.

Futhermore, the crystallite sizes of the phases were calculated from the X-ray diffractograms using the Scherrer formula, shown in equation (3.1).

$$t = \frac{0.9\lambda}{B cos\theta_B} \tag{3.1}$$

Here, t represents the crystallite size to be calculated, λ is the wavelength of the X-ray source (λ_{Cu}=1.54Å), B is the full-width half-maxima of the corresponding X-ray peak and θ_B is the Bragg angle of the corresponding peak.

3.3.2 Thermogravimetric analysis (TGA)

Thermal analyses were performed for determination of the mass changes on pyrolysis under inert atmosphere as well as on oxidation. Thermogravimetric tests were done in a Netzsch STA/TG-DSC instrument of PMPS and doped PMPS in argon atmosphere to understand the phase evolution. TGA was also performed on samples pyrolyzed at 1500°C with a ramp rate of 10°C/min under oxygen atmosphere to study the behavior of the ceramics upon oxidation.

3.3.3 Infrared Spectroscopy (FTIR)

Fourier transform infrared (FTIR) spectra was measured to identify any structural modification of SiOC backbone on addition of dopant ion. The samples were mixed with KBr in a ratio of 1:10 and was finely ground in a mortar. The mixture was pressed using a hydraulic press into a thin clear pellet. The pellet was inserted into the IR sample holder and the spectrum was run between 4000 and 400 cm^{-1} on a PerkinElmer Spectrum One FTIR spectrometer.

3.3.4 Transmission Electron Microscopy (TEM)

To confirm the crystalline phases in the SiOC matrix after polymer-to-ceramic transformation, transmission electron microscopy (TEM) was performed on the pyrolyzed samples. The powdered samples were dispersed in isopropyl alcohol and a drop of the solution was deposited on a carbon coated copper grid (300 mesh, Ted Pella, USA). The copper grid was allowed to dry. The grid was then placed in the sample holder for analysis.

TEM was performed by a 300 kV microscope (FEI, Technai™ G2) with a field emission electron gun. Bright field imaging and high resolution imaging was performed on the prepared samples.

For analysis of the TEM micrographs, Gatan DigitalMicrograph® software was used. The lattice fringes were calculated applying the fast Fourier-transform (FFT) algorithm on a

selected area over the micrograph of the lattice fringes in the crystallite. After computation, the fringe width was measured from the inverse FFT images derived from the micrograph.

Chapter 4

Results and Discussion

4.1 Thermal and phase evolution in polysilsesquioxane

Like poly(methyl phenyl)silsesquioxane (PMPS) polymer, poly(methyl)silsesquioxane (PMS) polymer is a methyl silicone resin with a high reactivity, and and the derived ceramics has heat resistance properties. Thermal characterizations and phase analysis were performed on the PMS and PMPS powders. These characterizations would act as a reference to qualify and quantify the effectiveness of the dopant atom (Zr or Ti) on the polymer derived silicon oxycarbide.

4.1.1 Silica content in polysilsesquioxane

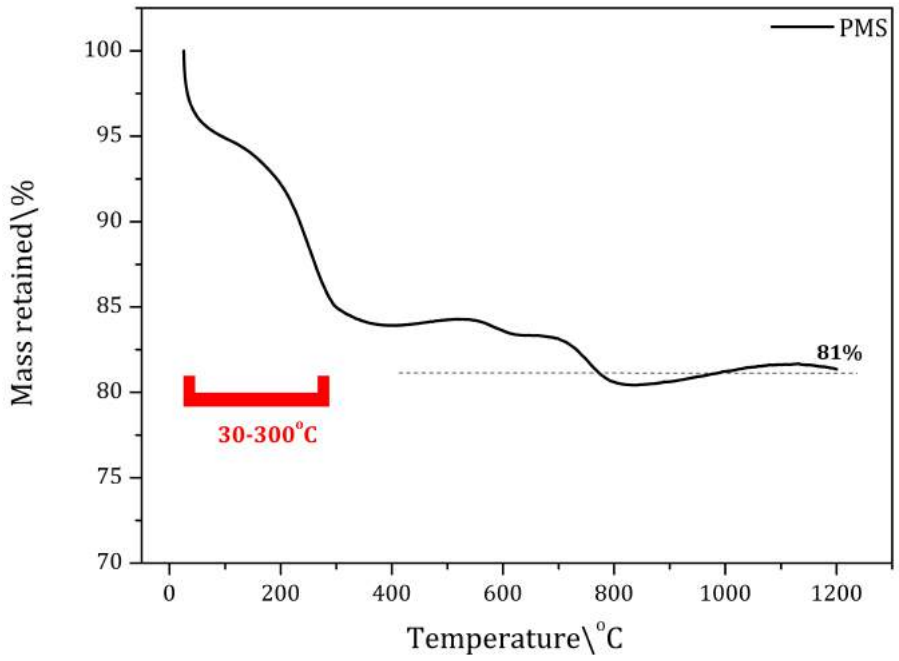

Figure 4.1: Mass loss in PMS polymer under air atmosphere

Figure 4.1 represents the mass loss in the pure PMS polymer in air atmosphere measured by thermogravimetric test. It shows the polymer-to-ceramic transformations that the PMS

polymer undergoes upon pyrolysis. It can be observed that the mass loss upon pyrolysis takes place predominantly in three stages. The polymer undergoes a major loss initially. This initial loss of ∼14% up to 300°C can be attributed to the loss of moisture and methane from the sample. The loss in the second stage, i.e., in the temperature regime of 300−800°C, is low, ∼2%. This loss corresponds to the loss of methane which was still in the system from the first stage. Beyond 800°C, the slope of the curve is somewhat constant, i.e., losses are minimal and are negligible. This stage suggests that all the organic has been converted to oxide phases, effectively SiO_2. This can be considered as the ceramic yield of the polymer which is ∼81% for the pure PMS polymer.

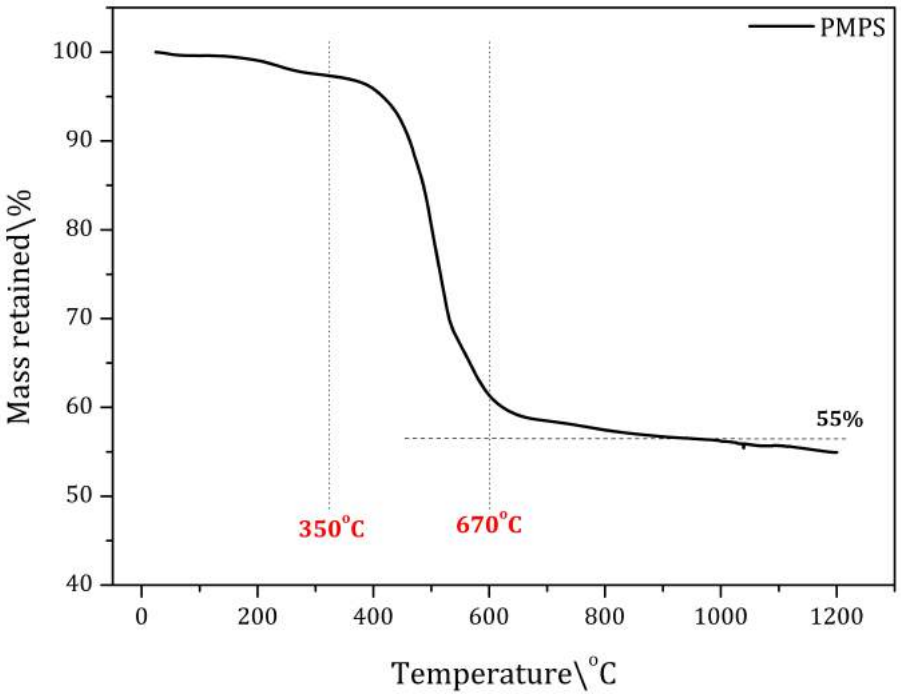

Figure 4.2: Mass loss in PMPS polymer under air atmosphere

Figure 4.2 represents the mass loss in the pure PMPS polymer under air atmosphere measured by thermogravimetric test. Similar to the PMS system, the mass loss upon pyrolysis takes place predominantly in three stages. There is an initial loss of ∼ 4% up to 350°C which can be attributed to the loss of moisture absorbed by the sample. Between 350−670°C, there is a drastic change in the mass of the polymer, i.e., ∼40%. A cross-linked PMPS would have a basic structure of $[-SiO_2-CH_3]+[Ph-SiO_2-]$ where Ph is the phenyl group. Upon pyrolysis, the phenyl group will be cleaved off from the $[Ph-SiO_2-]$ structure [79]. The drastic change between 350−670°C can be attributed to this loss of phenyl group. After these losses, the product that remains is $SiO_xC_yH_z$. With increase in temperature, further losses of hydrogen take place, leaving behind SiO_xC_y ceramic [79]. Beyond 670°C, the slope of the curve is somewhat constant. All the organic has been converted to oxide phases, effectively SiO_2. This can be considered as the ceramic yield of the polymer which

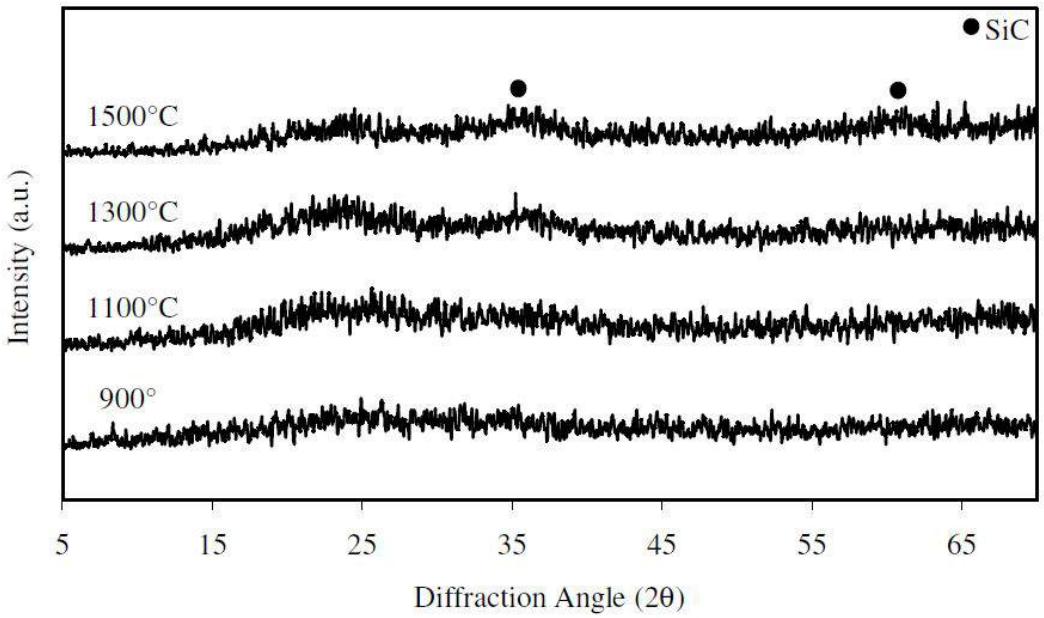

Figure 4.3: X-ray diffractograms of undoped poly(methyl)silsesquioxane pyrolyzed under Ar atmosphere at different temperatures [49].

is ∼55% for the pure PMPS polymer.

4.1.2 Phase analysis

Similar to the preparation of the doped poly(methyl phenyl)silsesquioxane ceramics (section 3.2), the as purchased polymer powders (PMS and PMPS) were cross-linked by addition of the cross-linking agent, triethanolamine (TEA), at 350°C for 2 hours in a muffle furnace. The resulting cross-linked powders were pyrolyzed under inert atmosphere at various temperatures. XRD analysis were performed on these pyrolyzed polymers to study the phases evolved and both of their X-ray diffractograms were compared.

Figure 4.4 shows the XRD patterns of the undoped poly(methyl)silsesquioxane pyrolyzed under inert argon atmosphere at elevated temperatures of 900−1500°C. It shows the phases formed in the ceramic upon pyrolysis. As it can be seen from the Figure 4.3, the silicon oxycarbide ceramic remains effectively amorphous in the entire range of the pyrolysis temperature.The β-SiC phase with characteristic peaks at diffraction angles of 36° and 60° (JCPDS #73-1665) are still in the amorphous SiOC network. Even at a temperature of 1500°C the carbide phase has not separated out from the matrix to form a crystalline phase.

Figure 4.4 shows the XRD patterns of the undoped poly(methyl phenyl)silsesquioxane pyrolyzed under inert argon atmosphere at elevated temperatures of 900−1500°C. The phases formed upon pyrolysis of PMPS can be studied from these X-ray diffractograms. Up to the pyrolysis temperature of 1200°C, the silicon oxycarbide ceramic retains its amorphous structure (Figure 4.4) . These amorphous XRD patterns are characteristics of SiO_xC_y

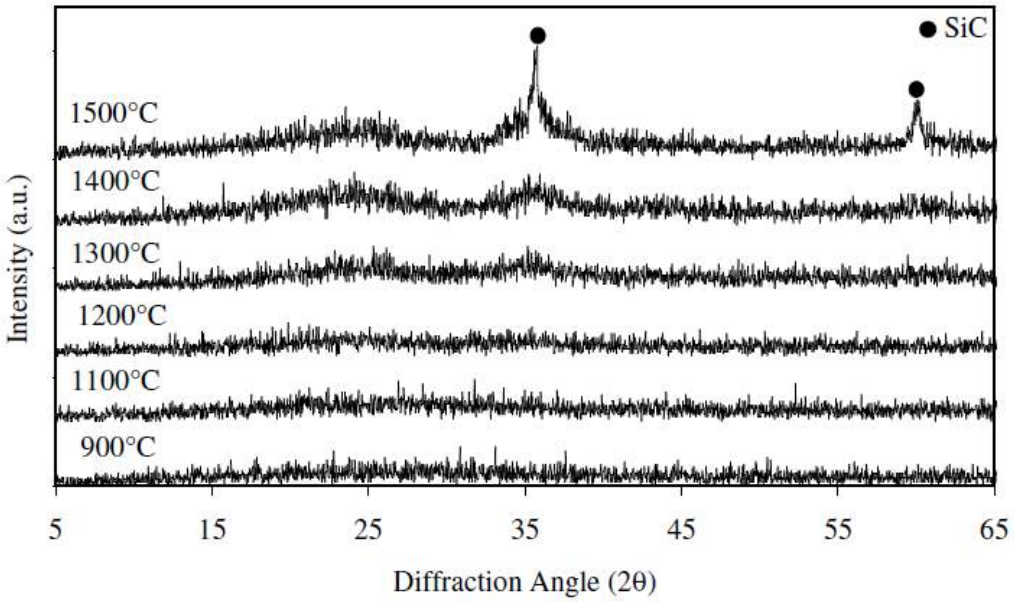

Figure 4.4: X-ray diffractograms of undoped poly(methyl phenyl)silsesquioxane pyrolyzed under Ar atmosphere at different temperatures [49].

ceramics. Broad peaks are vaguely visible at 1300°C which become quite distinct at 1400°C. The broad humps pinch off and phase separate to crystalline β-SiC whose characteristic peaks are at 36° and 60° (JCPDS #73-1665).

4.1.3 Remarks

The PMS polymer has a low mass loss upon pyrolysis under air, thus a high ceramic yield. This asserts that the carbon content in the polymer is low. On comparison with PMS, PMPS polymer thus has a high carbon content, since upon oxidation there is ∼45% mass loss which is due to loss of carbon from the polymer. Thus PMPS is chosen for investigations, citing its high carbon content.

Moreover, since the PMPS polymer phase separates into β-SiC upon pyrolysis under argon atmosphere at elevated temperatures, formation of this carbide phase can also be expected in the ceramic when doped with metal ions.

4.2 Zr-doped poly(methyl phenyl)silsesquioxane

4.2.1 Phase formation

Figure 4.5 shows the XRD pattern of Zr doped SiOC ceramic pyrolyzed under inert argon atmosphere at (a) 1000°C, (b) 1100°C and (c) 1500°C for 2 hours. It presents the effect of the Zr metal ion on the phase formation during the pyrolysis and formation of the SiZrOC ceramic. Phase formation at 1000°C and 1100°C in the SiZrOC ceramics for a Zr ion

concentration of 5, 10 and 20 mol% is depicted in Figure 4.5a and 4.5b.

The XRD patterns for both the temperatures are nearly the same. The ceramic stays in the amorphous state at a Zr concentration of 5 mol%. Comparison of the 5 mol% Zr concentration at both the temperatures shows that the low intense broad peaks at 1000°C have slightly pinched off. This suggests that crystallization started at 1100°C for 5 mol% Zr which was not possible at a 1000°C. With increase in Zr concentrations, the SiZrOC ceramic phase separates into tetragonal zirconia (JCPDS #79-1769). The only crystalline phase formed at 1000°C and 1100°C in the SiZrOC ceramics is t-ZrO_2. Moreover, the doublet at ∼35°, which is a characteristic peak of t-ZrO_2, cannot be resolved at the Zr doped SiOC pyrolyzed at 1000°C (Figure 4.5a), while the doublets at 50° and 60° (JCPDS #79-1769) are very faintly visible in both the samples pyrolyzed at 1000°C and 1100°C. This is probably due to the low crystallite sizes of the t-ZrO_2 at these temperatures.

With an anticipation of formation of carbide phases, especially zirconium carbide, at elevated temperatures, the SiZrOC ceramics were also pyrolyzed at 1500°C. Figure 4.5c shows the XRD pattern of the SiZrOC ceramics pyrolyzed at 1500°C. At this temperature, fully crystalline phases are formed. Apart from a single peak at 22.5°, which is attributed to SiO_2 (JCPDS #76-0941), the phases formed are that of tetragonal and monoclinic zirconia, mainly t-ZrO_2. It is also evident from Figure 4.5c that crystallization of t-ZrO_2 is promoted with increase in the Zr concentration since the t-ZrO_2 peak at 30° becomes more pronounced as the dopant concentration increases.

Moreover, the crystallite size of the t-ZrO_2 was calculated using the Scherrer equation. The respective crystallite sizes of ZrO_2 in the samples with highest Zr concentration, i.e., 20 mol% Zr, have been tabulated in Table 4.1. It was found that the crystallite size of t-ZrO_2 increased with increase in pyrolysis temperature which is intuitive.

Table 4.1: Crystallite sizes of t-ZrO_2 and m-ZrO_2 in SiZrOC at different temperatures

Temperature (°C)	t-ZrO_2 (nm)	m-ZrO_2 (nm)
1000	3.2	–
1100	5.7	–
1500	40.1	26.9

4.2.2 Microstructure

Figure 4.6 shows the microstructure of SiZrOC ceramics with a Zr concentration of 20 mol%, pyrolyzed at 1000°C. It was clear from the XRD patterns of the sample (figure 4.5a) about the presence of crystalline t-ZrO_2 phase in an amorphous matrix. To corroborate this fact, the microstructure of the 1000°C pyrolyzed 20 mol% Zr doped SiOC were characterized by TEM.

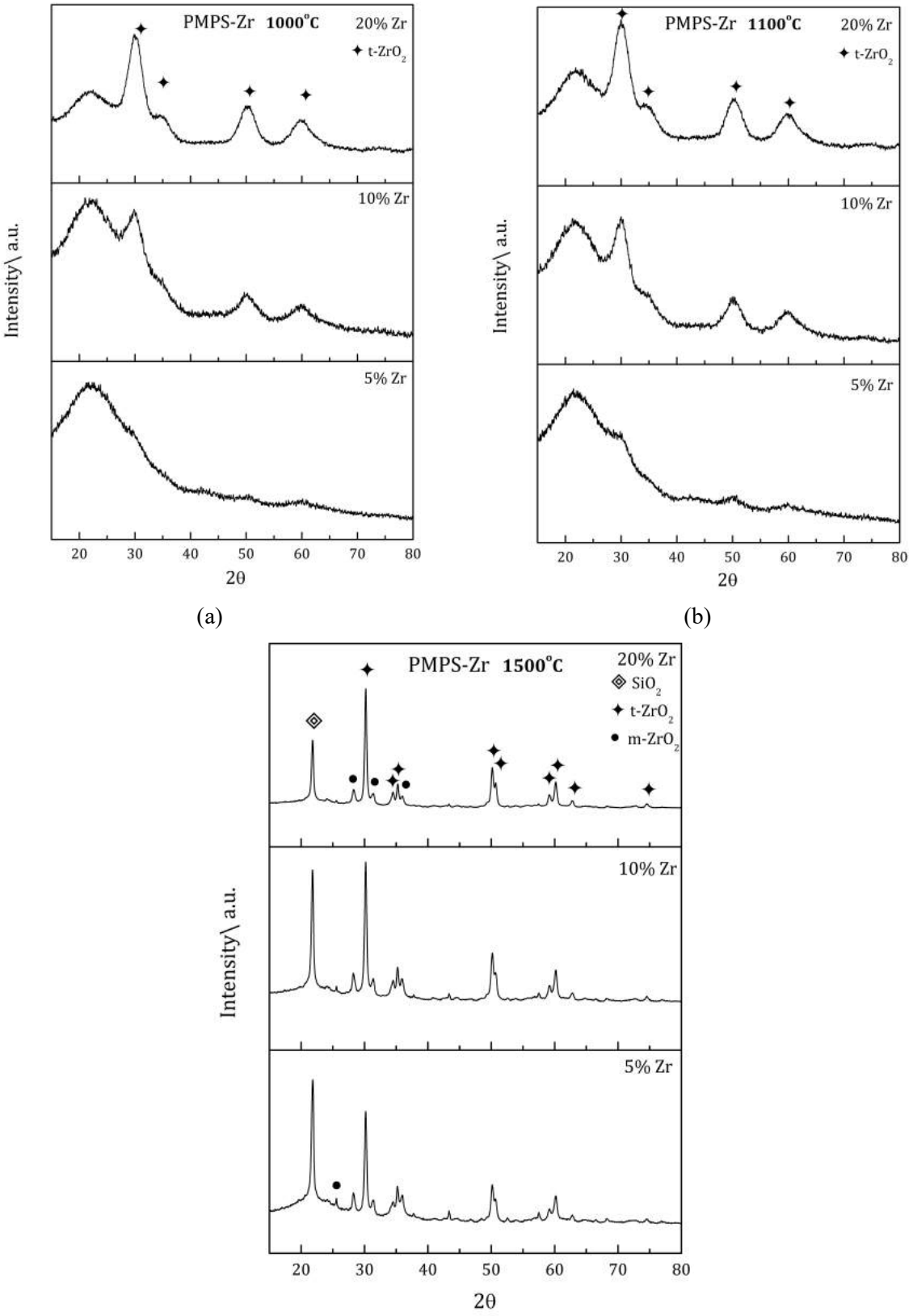

Figure 4.5: X-ray diffractograms of Zr doped SiOC ceramic pyrolyzed at (a) 1000°C, (b) 1100°C and (c) 1500°C under an inert Ar atmosphere for 2 hours

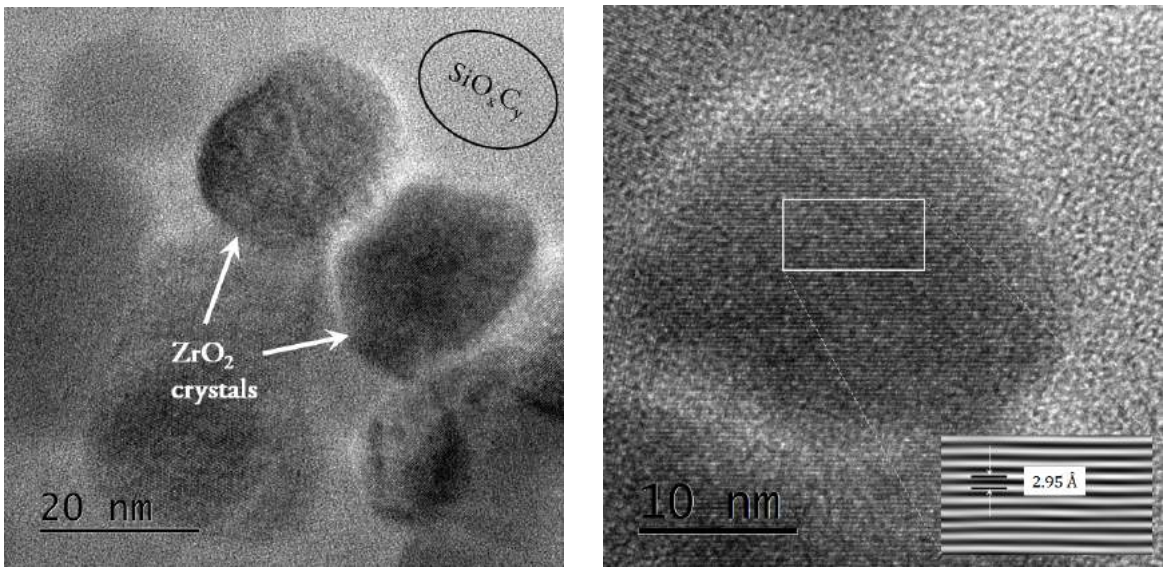

(a) (b)

Figure 4.6: HRTEM micrographs of SiZrOC ceramics pyrolyzed at 1000°C, (a) t-ZrO_2 dispersed in SiO_xC_y matrix, and (b) measurement of the lattice fringe width with a inverse fast Fourier-transform inset

Figure 4.6a confirms about the distribution of ZrO_2 crystals in the amorphous SiO_xC_y matrix. This is agreement with the XRD pattern (Figure 4.5a). To corroborate the t-ZrO_2 phase formation, which was established by the XRD patterns, the width of the lattice fringes of a crystal was computed using a fast Fourier transform (FFT) algorithm. The TEM micrograph shown in Figure 4.6b represents this calculation where the computed inverse FFT is inset in the micrograph. Measurements showed that the lattice fringe width was 2.95Å which confirms with the d-spacing of (101) plane of t-ZrO_2 (JCPDS #79-1769), thus confirming t-ZrO_2 phase.

4.2.3 Remarks

The SiOC system phase separated into β-SiC upon pyrolysis at 1500°C (Figure 4.4), but no such peaks corresponding to β-SiC was found in the SiZrOC system. The system only produced metal oxides with the absence of any carbide phase.

The HRTEM micrographs of of SiZrOC ceramics pyrolyzed at 1000°C (Figure 4.6a) show that the ZrO_2 nanocystals have a size of $\sim$20 nm, while the crystallite sizes calculated from the Scherrer equation show a low value. This discrepancy is due to the peak broadening in the X-ray diffractograms of the 1000°C (Figure 4.5a). The ZrO_2 has not fully crystallized, resulting in a broad peak due to amorphous nature. This broadening of the peak gives a decreased value upon calculation of the crystallite sizes while the HRTEM micrographs show a fully crystallized ZrO_2.

In the absence of a stabilizer, for the t-ZrO_2 phase to be stable, the crystallite size of the

phase should remain below about 30 nm [80]. In the present work, the t-ZrO_2 nanocrystals were found to be stable even at 40 nm in the samples pyrolyzed at 1500°C and cooled to room temperature. This can be explained by the fact that the growth of these t-ZrO_2 nanocrystals can be considered to be a crystal growth in an otherwise glassy matrix. Such type of growth produces spherical or ellipsoidal crystals [81]. Here, these crystals are embedded in the ceramic SiOC matrix, thus preventing the t-ZrO_2 nanocrystals to transform into its other stable polymorphic states. Moreover, these spherical nanocrystals do not have any edges which would otherwise act as stress concentrators, thus inducing polymorphic transformations.

4.3 Ti-doped poly(methyl phenyl)silsesquioxane

4.3.1 Thermal behavior

To study the mass loss upon pyrolysis of pure SiOC system under inert argon atmosphere, thermogravimetric (TG) measurements were performed. In order to study the effect of doped Ti ions on the SiOC system, the mass loss data of pure SiOC system was compared with that of the SiTiOC system. Figure 4.7 shows the mass loss in the pure SiOC system and the SiTiOC ceramic as well, pyrolyzed under inert argon atmosphere where the Ti concentration is 20 mol%.

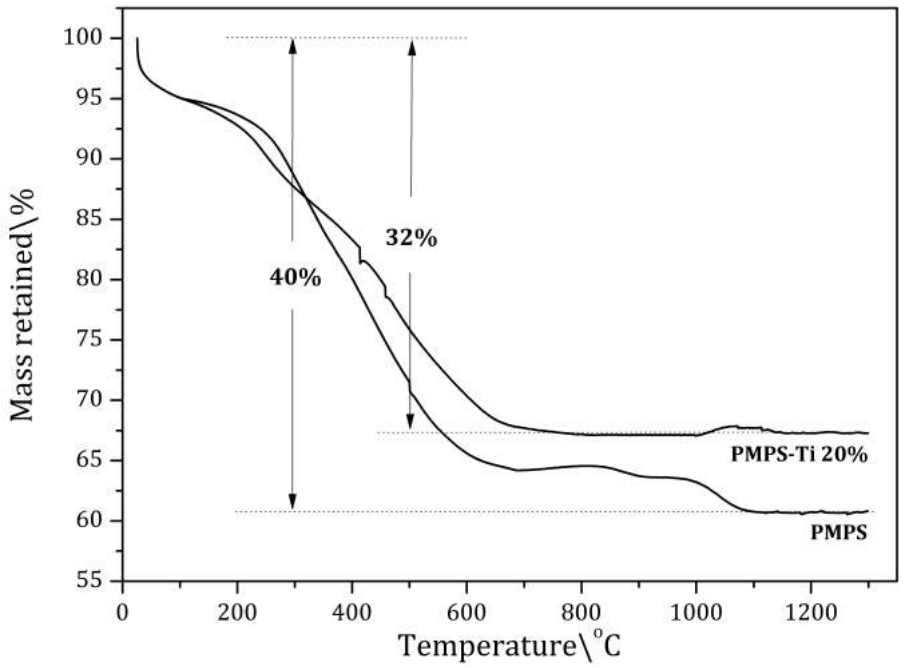

Figure 4.7: Mass loss in pure PMPS and Ti (20 mol%) doped PMPS pyrolyzed under inert Ar atmosphere

It is evident from the Figure 4.7 that the mass loss in the pure SiOC ceramic is 40% which reduced to 32% after doping of Ti metal. In both of the systems, there is a significant

loss up to 600°C. This can be attributed to the loss of moisture and the phenyl group from the PMPS polymer, as explained in section 4.1.1. A further loss of ∼5% is observed in the PMPS sample whereas effectively, there is no mass loss beyond 700°C. This additional loss can be attributed to the unreacted materials in the PMPS polymer that did not decompose in the first stage of pyrolysis, i.e., up to 700°C. This loss is due to release of methane from the PMPS system. The Ti doped PMPS attains stability to thermal decomposition beyond 700°C perhaps due to the incorporation of Ti into the tetrahedral Si network of the polymer [4]. Moreover, the Ti ions interact with free carbon in the structure, presumably forming carbides. This is in agreement with the XRD patterns (Figure 4.8) where the titanium carbide remains amorphous in the SiTiOC network and starts phase separating at temperatures beyond 1200°C.

4.3.2 Phase formation

Figure 4.8 shows the XRD pattern of Ti doped SiOC ceramic pyrolyzed in an inert argon atmosphere at (a) 1000°C, (b) 1200°C, (c) 1300°C and (d) 1500°C for 2 hours. It projects the effect of the Ti metal ion on the phase formation during the pyrolysis and formation of the SiTiOC ceramic.

Figure 4.8a represents the phases formed when the doped polymer was pyrolyzed at 1000°C. It is quite evident that the phase structure of the ceramic remains amorphous, even at the highest concentration of the dopant ion. The broad hump at 20° corresponds to the SiO_2 phase (JCPDS #76-0941) which has not been phase separated and is in the amorphous SiO_xC_y. This feature is consistent with the existence of SiO_2 nanodomains, with sizes in the range of $1-2$ nm, typically a few molecular unit clusters. There are two minor humps at 36°and ∼42°. The hump at 36° is vaguely visible in Ti concentrations of 15 and 20 mol% and it corresponds to the β-SiC which is in the amourphous state. The later minor hump, i.e., the hump at ∼42° corresponds to carbide nuclei formed by the doped Ti ions which is also in present in an amorphous state.

Figure 4.8b represents the phases formed when the doped polymer was pyrolyzed at 1200°C. The peaks have relatively become narrower, thus depicting the amorphous-to-crystalline transformation. The minor peaks have become sharper showing the formation of β-SiC (JCPDS #73-1665) and TiC (JCPDS #71-0298) at 36° and 42° respectively. The SiO_2 phase is still in the amorphous state, even at the highest concentration of Ti ion.

Figure 4.8c represents the phases formed when the doped polymer was pyrolyzed at 1300°C. At 1300°C, SiO_2 phase has begun phase separation into crystalline state even at low concentrations of Ti. β-SiC and TiC have also crystallized at this temperature. As the concentration of Ti increases from 5 mol% to 20 mol%, the phase separation to crystalline phase gradually increases and coarsening of the crystals takes place. The gradual pinching

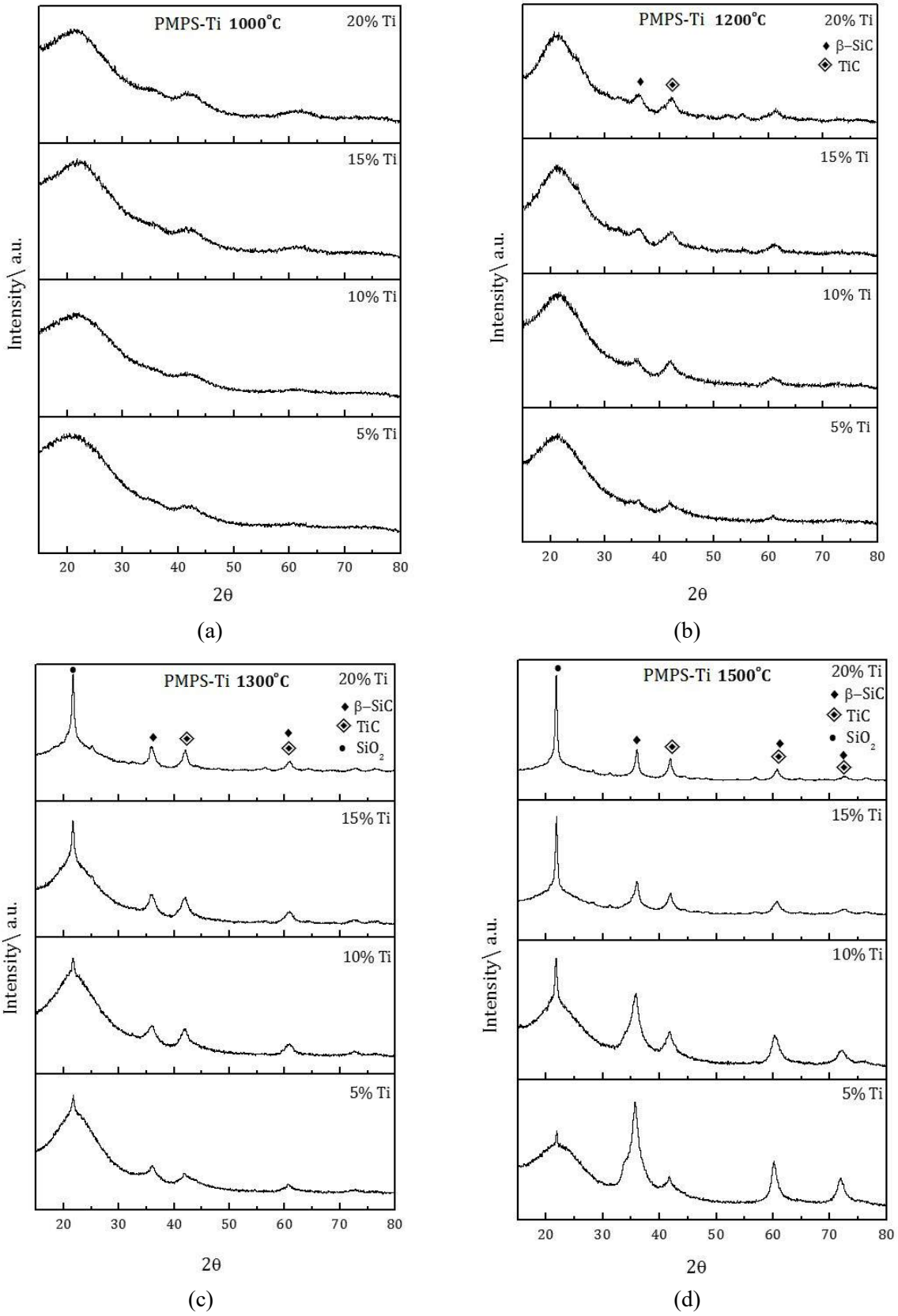

Figure 4.8: X-ray diffractograms of Ti doped SiOC ceramic pyrolyzed at (a) 1000°C, (b) 1200°C, (c) 1300°C and (d) 1500°C under an inert Ar atmosphere for 2 hours

Table 4.2: Crystallite sizes of the phases separated in SiTiOC at different temperatures

Temperature (°C)	SiO_2 (nm)	β-SiC (nm)	TiC (nm)
1200	–	4.4	4.8
1300	12.8	8.3	8.1
1500	17.1	12.2	11.5

off of a peak with a broad background at ∼20° of 2θ indicates that some of the SiO_2 nanodomains have started to grow in size, while a majority of the SiO_2 phase still remains as few molecular clusters. For 20 mol% Ti doped SiOC at 1300°C, however, complete phase separation occurs.

Figure 4.8d represents the phases formed when the doped polymer was pyrolyzed at 1500°C. At this temperature, all the phases, i.e., SiO_2, β-SiC and TiC are in crystalline state. It can be seen from the XRD pattern that the significant coarsening of the SiO_2 crystallites take place on increasing the dopant ion concentration. The β-SiC peak at 36° seems to decrease in intensity due to this reason. It is also evident that coarsening of TiC crystallites take place as the TiC peak at 42° intensifies with increase in Ti ion concentration.

From the XRD patterns shown in Figure 4.8, it was found that the the crystallisation of β-SiC and TiC started at 1200°C. The sample pyrolyzed at this temperature is of importance since the β-SiC and TiC crystallites would be distributed in the amorphous SiOC matrix where the Si ion has not phase separated from the ceramic to form SiO_2 crystals. These samples were characterized using transmission electron microscope (TEM) to corroborate this fact.

Moreover, Scherrer formula was used to calculate the crystallite sizes of the phases that separated out in the SiTiOC ceramic. Table 4.2 tabulates the respective crystallite sizes of SiO_2, β-SiC and TiC in the SiTiOC ceramics. It can be inferred from the graph that there is a growth in the sizes of the crystals with increase in temperature. It must be noted that the growth in crystallite size of β-SiC is higher than that of TiC. This pronounced effect is presumably due to the fact that pure PMPS phase separates to β-SiC at 1500°C (refer section 4.1.2).

4.3.3 Chemical structure

Fourier transform infrared spectroscopy (FTIR) was used to investigate the thermal conversion from organic (cross-linked) silsesquioxane network into the inorganic ceramic structure. Figure 4.9 represents the FTIR analysis of 350°C cross-linked PMPS, Ti-doped cross-linked PMPS and Ti-doped PMPS samples pyrolyzed at 1100°C, 1300°C and 1500°C. The streching and bending vibrations of O−H bond have been indexed to the bands at around 3434 cm^{-1} and 1653 cm^{-1} respectively [60]. It can be seen that the O−H bond has depleted

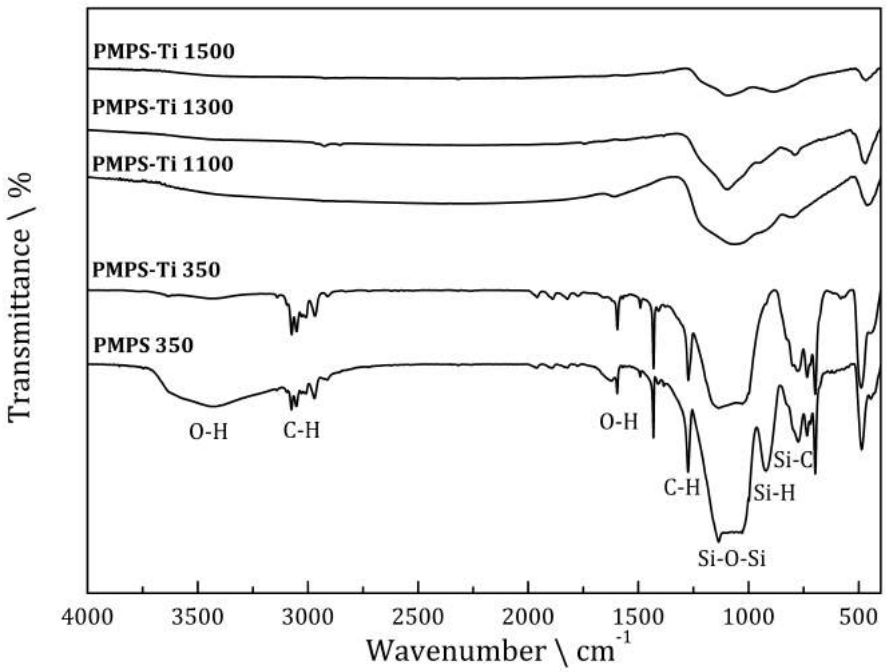

Figure 4.9: FTIR of cross-linked pure and Ti doped PMPS alongwith pyrolyzed Ti doped PMPS, pyrolyzed at various temperatures

in the spectra of the pyrolyzed samples. This is due to the polymer-to-ceramic conversion. The presence of C−H vibration band in the spectra of the cross-linked samples is due to the methyl group. These vibration bands which are present at 2968 cm^{-1} and 1272 cm^{-1} are predominantly absent in the pyrolyzed samples due to the volatization of the hydrocarbons from the structure.

The vibration band of Si−O−Si bond in the range of 1000 and 1140 cm^{-1} is split into two bands at 1028 cm^{-1} and 1134 cm^{-1} in both the cross-linked samples. This shows the high degree of polymerization in the cross-linked samples which is due to the addition of TEA for cross-linking of the precursors. But at higher pyrolysis temperatures, these split bands merge into a single band at 1096 cm^{-1}. This is due to the phase separation of SiO_2 from the structure [82]. Moreover, the Si−H band at 922 cm^{-1} present in the cross-linked PMPS sample is depleted in the spectra of th cross-linked Ti doped PMPS and is replaced by a minute band which is barely visible. This is due to the presence of $Ti(O^nPr)_4$ which facilitates the formation of Si−O−Ti bond.

4.3.4 Microstructure

Figure 4.10 shows the high resolution TEM micrographs of SiTiOC ceramics pyrolyzed at 1200°C with a Ti concentration of 20 mol%. Figure 4.10a shows the distribution of fine crystallites in an otherwise glassy matrix. This can be inferred from the grayish spots distributed in a matrix with a different contrast than these spots. The width of the lattice fringes of a crystal was computed using a fast Fourier transform (FFT) algorithm. The TEM

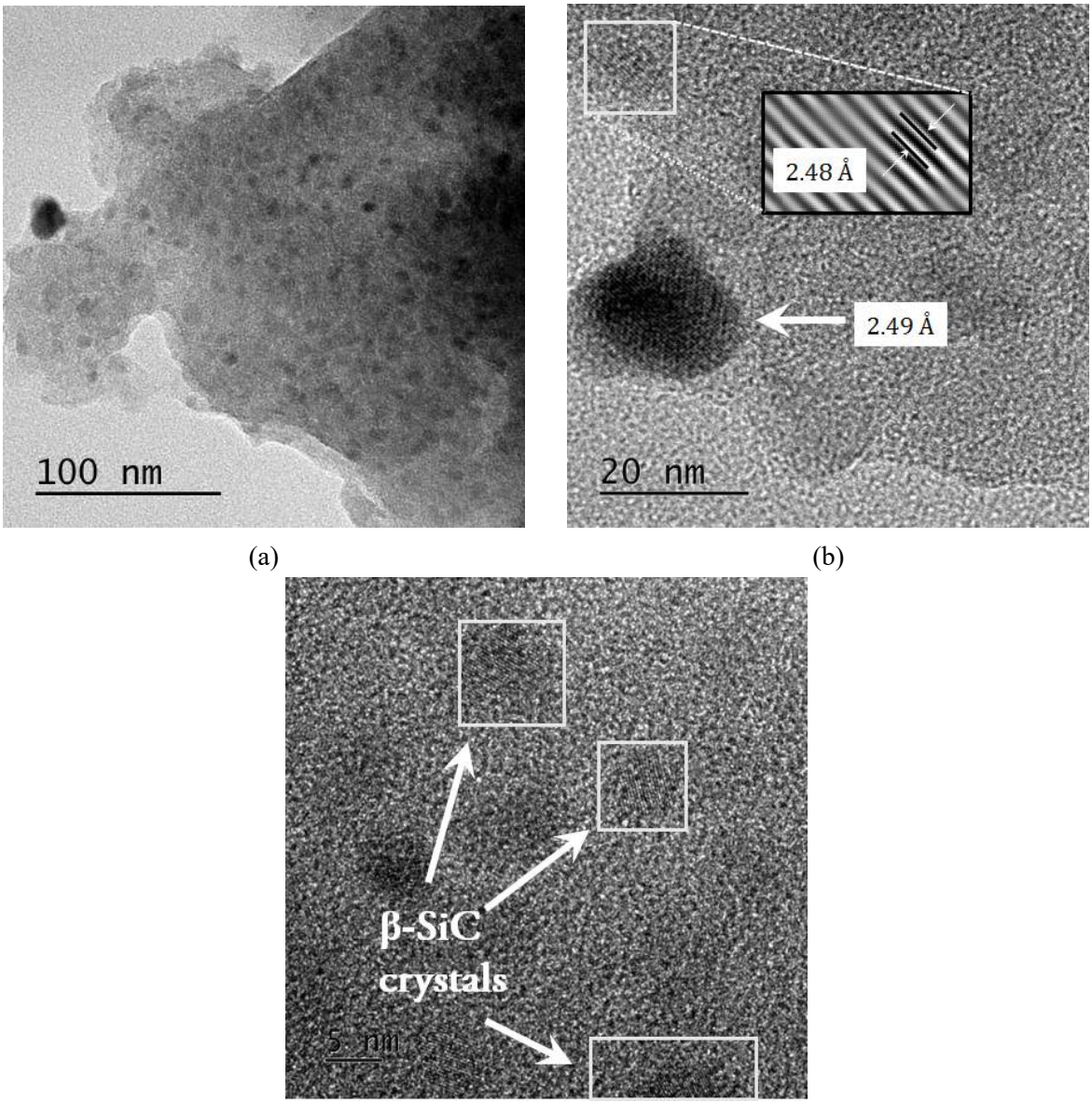

(a) (b)

(c)

Figure 4.10: HRTEM images of SiTiOC ceramics pyrolyzed at 1200°C, (a) the general microstructure of the SiTiOC, (b) measurement of lattice fringe width with a inverse fast Fourier-transform inset, and (c) the distribution of β-SiC nanocrystals in the SiOC matrix

micrograph shown in Figure 4.10b represents this calculation where the computed inverse FFT is inset in the micrograph. Measurements showed that the lattice fringe width was 2.49Å which confirms with the d-spacing of (111) plane of TiC (JCPDS #71-0298), thus confirming TiC phase. The nanocrystals marked in Figure 4.10c have been identified to be β-SiC from the lattice fringe width. Similarly, using the FFT algorithm (the inverse FFT image has not been show in the micrograph) the lattice width was indexed with the d-spacing of (111) plane (i.e., 2.51Å) of β-SiC (JCPDS #73-1665), confirming β-SiC phase and thus in accordance with the X-ray diffractograms (Figure 4.8b).

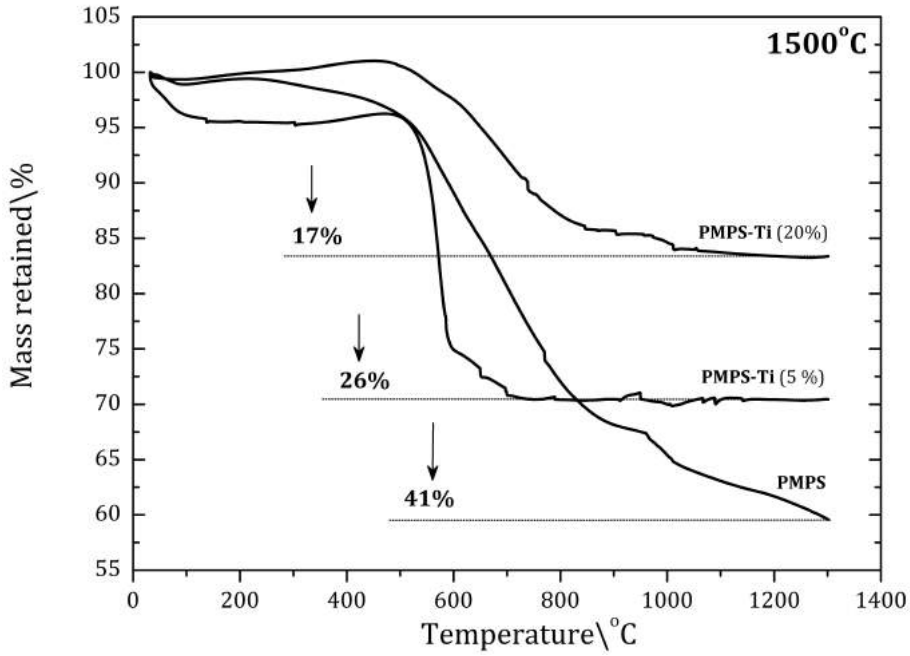

Figure 4.11: Oxidation tests by thermogravimetric measurements under flowing oxygen atmosphere of SiOC, 5 mol% Ti doped SiOC and 20 mol% Ti doped SiOC samples, all pyrolyzed at 1500°C

4.3.5 Oxidation tests

Oxidative analysis of the SiTiOC ceramic was carried out by TG measurements where the 1500°C pyrolyzed Ti doped sample was analyzed. Although there was a phase separation of SiO_2 from the amorphous network, the 1500°C pyrolyzed sample had a higher content of β-SiC and TiC. This can be referred from the XRD patterns (Figure 4.8) where the corresponding peak intensity of β-SiC and TiC was relatively higher for the 1500°C pyrolyzed sample compared to other temperatures.

Figure 4.11 represents the oxidations tests done on the SiTiOC ceramics pyrolyzed at 1500°C where the dopant ion concentration is 5 and 20 mol%. This has been compared with the oxidation tests conducted on pure SiOC, cross-linked at 350°C and pyrolyzed at 1500°C.

The thermogravimetric (TG) measurements up to 1300°C under oxygen atmosphere shows that the 1500°C pyrolyzed PMPS suffers a mass loss of 41%. This is due to the loss of free carbon present in the structure. Upon incorporation of 5 mol% Ti in the SiOC structure, the mass loss on oxidation of the SiTiOC reduces to 26%. This reduction in the mass loss is due to the utilization of the free carbon present in SiOC system to form carbide phases, here, titanium carbide. With increase in Ti mol% to 20 mol%, the mass loss is further reduced to 17%. This 9% reduction is due to the formation and growth of TiC phase in the SiTiOC structure.

4.4 *Ab initio* calculations

To answer on the possible structure of the PDC network upon doping, i.e., the placement of the doped atoms in the amorphous network, Terauds and Raj [4] had put forth a hypothesis that the doped atoms substitutes for silicon in the network. Figure 4.12 illustrates the amorphous tetrahedral structure before and after the substitution by dopant atoms. The shown model is based upon the possible formation of three Si−O bonds since the precursor polymer has a silsesquioxane.

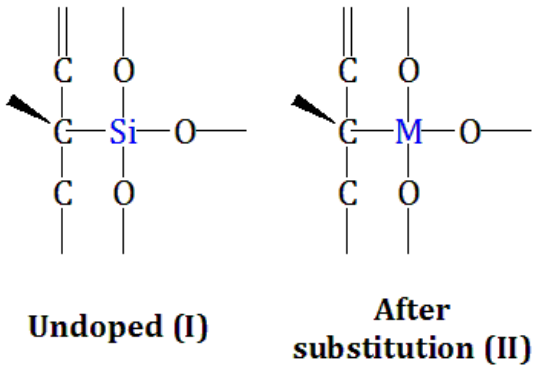

Figure 4.12: Molecular states before and after dopant atom (M) substitution at the center of tetrahedral bonding

Basing upon this hypothesis, the difference in the enthalpy between Si and M (where M=Zr or Ti) being bonded to C and O can be calculated by a simple bond-counting approach. The difference in the energy between the doped and the undoped state can be calculated from the equation (4.1).

$$\begin{aligned}\Delta G_{M/Si} &= \Delta G_{II} - \Delta G_I \\ &= 3(\Delta H_{M-O} - \Delta H_{Si-O}) + (\Delta H_{M-C} - \Delta H_{Si-C}) + RTln(\frac{a_M}{a_{Si}})\end{aligned} \tag{4.1}$$

Here, ΔG represents the free energy, ΔH is the enthalpy of the bonds formed from atomic species, M is the dopant atom (Zr or Ti), a_M and a_{Si} are the activities of the dopant atom and Si respectively while R and T carry their usual meanings. To estimate $\Delta H_{M/Si}$ of the mixed-bond configuration, considering the enthalpy terms only, equation (4.1) can be written as:

$$\Delta H_{M/Si} = 3(\Delta H_{M-O} - \Delta H_{Si-O}) + (\Delta H_{M-C} - \Delta H_{Si-C}) \tag{4.2}$$

The bond energies are presented in Table 4.3 assuming quadrivalent bonding. Substituting the respective metal-oxide and metal-carbide bond enthalpies in the resulting equation (4.2), the $\Delta H_{M/Si}$ of Zr and Ti doped system has been calculated and tabulated in Table 4.3. It should also be noted that since the reactions involving the formation of the metal (Si, Zr and Ti) oxides and the carbides are exothermic in nature, the enthalpy of formation is attributed

a negative sign.

Table 4.3: Bond energies (kJ/mol) in a melt and their respective bond enthalpy

Element	M-O	M-C	$\Delta H_{M/Si}$
Si	-461	-294	$\times$
Zr	-529	-361	-271
Ti	-462	-326	-35

It is quite evident from the Table 4.3 that the change in enthalpy upon substitution of Si-centered mixed-bond tetrahedral units by Zr- and Ti-centered units has negative values. This suggests that the substitution is exothermic and thus energetically favorable.

Chapter 5

Conclusion

In an attempt to modify the silicon oxycarbide structure by incorporating transition metal elements such as Zr and Ti, the following conclusions were drawn out.

- Although the PMPS polymer had a low ceramic yield, complementally it was found to have a high carbon content. Thus, PMPS polymer was chosen for the present study.
- In the Zr doped SiOC system, no SiC phase was observed although pure SiOC phase separated to β-SiC at higher temperatures.
- SiO_2 growth occured in the Zr system from nanodomains to nanoparticles to big crystals.
- Crystallite sizes of t-ZrO_2 was calculated by Scherrer formula. It was observed that crystallite growth occured with increasing temperature.
- It was also found that the t-ZrO_2 was even stable at 1500°C which was counter intuitive.
- It was concluded from the Zr system that effectively no carbon of PMPS derived silicon oxycarbide is being used up, hence this gave the idea of incorporation of Ti.
- Ti system was found to be effective as carbide phases, namely silicon carbide and titanium carbide were formed.
- It was found out that upon incorporation of Ti, mass loss during oxidation reduced. Furthermore, with increase in concentration of Ti, mass loss on oxidation decreased.
- Microstructural analysis of both the samples through TEM studies revealed the dispersion of nanocrystals in the amorphous matrix of SiO_xC_y system.
- Finally, *ab initio* calculations were performed to support the hypothesis regarding the placement of these dopant atoms in the amorphous SiOC network.

References

[1] M. N. Rahaman, *Ceramic processing*. Wiley Online Library, 2006.

[2] P. Colombo, G. Mera, R. Riedel, and G. D. Sorarù, ‘‘Polymer-derived ceramics: 40 years of research and innovation in advanced ceramics,’’ *Journal of the American Ceramic Society*, vol. 93, no. 7, pp. 1805–1837, 2010.

[3] R. Sujith, A. B. Kousaalya, and R. Kumar, ‘‘Coarsening induced phase transformation of hafnia in polymer-derived Si–Hf–C–N–O ceramics,’’ *Journal of the American Ceramic Society*, vol. 94, no. 9, pp. 2788–2791, 2011.

[4] K. Terauds and R. Raj, ‘‘Limits to the stability of the amorphous nature of polymer-derived HfSiCNO compounds,’’ *Journal of the American Ceramic Society*, vol. 96, no. 7, pp. 2117–2123, 2013.

[5] Y. D. Blum, D. B. MacQueen, and H.-J. Kleebe, ‘‘Synthesis and characterization of carbon-enriched silicon oxycarbides,’’ *Journal of the European Ceramic Society*, vol. 25, no. 2, pp. 143–149, 2005.

[6] G. Gregori, H.-J. Kleebe, Y. D. Blum, and F. Babonneau, ‘‘Evolution of C-rich SiOC ceramics: Part II. Characterization by high lateral resolution techniques: Electron Energy-Loss Spectroscopy, High-Resolution TEM and Energy-Filtered TEM,’’ *Zeitschrift für Metallkunde*, vol. 97, no. 6, pp. 710–720, 2006.

[7] H.-J. Kleebe, G. Gregori, F. Babonneau, Y. D. Blum, D. B. MacQueen, and S. Masse, ‘‘Evolution of C-rich SiOC ceramics: Part I. Characterization by integral spectroscopic techniques: Solid-state NMR and Raman spectroscopy,’’ *Zeitschrift für Metallkunde*, vol. 97, no. 6, pp. 699–709, 2006.

[8] H.-J. Kleebe and Y. D. Blum, ‘‘SiOC ceramic with high excess free carbon,’’ *Journal of the European Ceramic Society*, vol. 28, no. 5, pp. 1037–1042, 2008.

[9] G. Mera, R. Riedel, F. Poli, and K. Müller, ‘‘Carbon-rich SiCN ceramics derived from phenyl-containing poly (silylcarbodiimides),’’ *Journal of the European Ceramic Society*, vol. 29, no. 13, pp. 2873–2883, 2009.

[10] T. Konegger, J. Torrey, O. Flores, T. Fey, B. Ceron-Nicolat, G. Motz, F. Scheffler, M. Scheffler, P. Greil, and R. K. Bordia, ‘‘Ceramics for sustainable energy technologies with a focus on polymer-derived ceramics,’’ in *Novel Combustion Concepts for Sustainable Energy Development*. Springer, pp. 501–533, 2014.

[11] S. Martínez-Crespiera, E. Ionescu, M. Schlosser, K. Flittner, G. Mistura, R. Riedel, and H. Schlaak, ‘‘Fabrication of silicon oxycarbide-based microcomponents via photolithographic and soft lithography approaches,’’ *Sensors and Actuators A: Physical*, vol. 169, no. 1, pp. 242–249, 2011.

[12] R. Riedel, G. Mera, R. Hauser, and A. Klonczynski, ‘‘Silicon-based polymer-derived ceramics: synthesis properties and applications–a review,’’ *Journal of the Ceramic Society of Japan*, vol. 114, no. 1330, pp. 425–444, 2006.

[13] R. Riedel, L. Toma, E. Janssen, J. Nuffer, T. Melz, and H. Hanselka, ‘‘Piezoresistive effect in SiOC ceramics for integrated pressure sensors,’’ *Journal of the American Ceramic Society*, vol. 93, no. 4, pp. 920–924, 2010.

[14] L. Toma, H.-J. Kleebe, M. M. Müller, E. Janssen, R. Riedel, T. Melz, and H. Hanselka, ‘‘Correlation between intrinsic microstructure and piezoresistivity in a SiOC polymer-derived ceramic,’’ *Journal of the American Ceramic Society*, vol. 95, no. 3, pp. 1056–1061, 2012.

[15] S. K. Behera and R. Raj, ‘‘Extreme-rate capable and highly stable SiCO–TiO_2 hybrids for Li ion battery anodes,’’ *Chemical Communications*, vol. 49, no. 83, pp. 9657–9659, 2013.

[16] J. Kaspar, G. Mera, A. P. Nowak, M. Graczyk-Zajac, and R. Riedel, ‘‘Electrochemical study of lithium insertion into carbon-rich polymer-derived silicon carbonitride ceramics,’’ *Electrochimica Acta*, vol. 56, no. 1, pp. 174–182, 2010.

[17] E. Ionescu, ‘‘Polymer-derived ceramics,’’ *Ceramics Science and Technology, Set*, pp. 457–500, 2012.

[18] P. Colombo, *Polymer derived ceramics: from nano-structure to applications*. DEStech Publications, Inc, 2010.

[19] G. Fritz and B. Raabe, ‘‘Bildung siliciumorganischer verbindungen. v. die thermische zersetzung von $Si(CH_3)_4$ und $Si(C_2H_5)_4$,’’ *Zeitschrift für anorganische und allgemeine Chemie*, vol. 286, no. 3-4, pp. 149–167, 1956.

[20] F. W. Ainger and J. M. Herbert, *The Preparation of Phosphorus-Nitrogen Compounds as Non-Porous Solids*. Academic press, New York, pp. 168–182, 1960.

[21] P. G. Chantrell and P. Popper, *Inorganic Polymers and Ceramics*. Academic press, New York, pp. 87–103, 1965.

[22] S. Yajima, J. Hayashi, and M. Omori, ‘‘Continuous silicon carbide fiber of high tensile strength,’’ *Chemistry Letters*, vol. 4, no. 9, pp. 931–934, 1975.

[23] S. Yajima, Y. Hasegawa, J. Hayashi, and M. Iimura, ‘‘Synthesis of continuous silicon carbide fibre with high tensile strength and high Young’s modulus,’’ *Journal of Materials Science*, vol. 13, no. 12, pp. 2569–2576, 1978.

[24] T. Rouxel, G.-D. Soraru, and J. Vicens, ‘‘Creep viscosity and stress relaxation of gel-derived silicon oxycarbide glasses,’’ *Journal of the American Ceramic Society*, vol. 84, no. 5, pp. 1052–1058, 2001.

[25] L. An, R. Riedel, C. Konetschny, H. Kleebe, R. Raj *et al.*, ‘‘Newtonian viscosity of amorphous silicon carbonitride at high temperature,’’ *Journal of the American Ceramic Society*, vol. 81, no. 5, pp. 1349–1352, 1998.

[26] R. Riedel, L. M. Ruswisch, L. An, and R. Raj, ‘‘Amorphous silicoboron carbonitride ceramic with very high viscosity at temperatures above 1500°C,’’ *Journal of the American Ceramic Society*, vol. 81, no. 12, pp. 3341–3344, 1998.

[27] S. Modena, G. D. Sorarù, Y. Blum, and R. Raj, ‘‘Passive oxidation of an effluent system: The case of polymer-derived SiCO,’’ *Journal of the American Ceramic Society*, vol. 88, no. 2, pp. 339–345, 2005.

[28] Y. Wang, W. Fei, and L. An, ‘‘Oxidation/corrosion of polymer-derived SiAlCN ceramics in water vapor,’’ *Journal of the American Ceramic Society*, vol. 89, no. 3, pp. 1079–1082, 2006.

[29] R. Riedel, A. Kienzle, W. Dressler, L. Ruwisch, J. Bill, and F. Aldinger, ‘‘A silicoboron carbonitride ceramic stable to 2000°C,’’ *Nature*, vol. 382, no. 6594, pp. 796–798, 1996.

[30] A. Saha and R. Raj, ‘‘Crystallization maps for sico amorphous ceramics,’’ *Journal of the American Ceramic Society*, vol. 90, no. 2, pp. 578–583, 2007.

[31] M. Kotani, A. Kohyama, and Y. Katoh, ‘‘Development of SiC/SiC composites by PIP in combination with RS,’’ *Journal of Nuclear Materials*, vol. 289, no. 1, pp. 37–41, 2001.

[32] K. Kaneko and K.-I. Kakimoto, ‘‘HRTEM and ELNES analysis of polycarbosilane-derived Si–C–O bulk ceramics,’’ *Journal of non-crystalline solids*, vol. 270, no. 1, pp. 181–190, 2000.

[33] C. L. Schilling, ‘‘Polymeric routes to silicon carbide,’’ *British polymer journal*, vol. 18, no. 6, pp. 355–358, 1986.

[34] X. Bao and M. Edirisinghe, ‘‘Different strategies for the synthesis of silicon carbide–silicon nitride composites from preceramic polymers,’’ *Composites Part A: Applied Science and Manufacturing*, vol. 30, no. 5, pp. 601–610, 1999.

[35] R. Wills, R. Markle, and S. P. Mukherjee, ‘‘Siloxanes, silanes, and silazanes in the preparation of ceramics and glasses,’’ 1983.

[36] S. Trassl, G. Motz, E. Rössler, and G. Ziegler, ‘‘Characterisation of the free-carbon phase in precursor-derived SiCN ceramics,’’ *Journal of non-crystalline solids*, vol. 293, pp. 261–267, 2001.

[37] G. Ziegler, I. Richter, and D. Suttor, ‘‘Fiber-reinforced composites with polymer-derived matrix: processing, matrix formation and properties,’’ *Composites Part A: Applied Science and Manufacturing*, vol. 30, no. 4, pp. 411–417, 1999.

[38] T. Michalet, M. Parlier, A. Addad, R. Duclos, and J. Crampon, ‘‘Formation at low temperature with low shrinkage of polymer/Al/Al_2O_3 derived mullite,’’ *Ceramics international*, vol. 27, no. 3, pp. 315–319, 2001.

[39] A. Kaindl, W. Lehner, P. Greil, and D. J. Kim, ‘‘Polymer-filler derived Mo_2C ceramics,’’ *Materials Science and Engineering: A*, vol. 260, no. 1, pp. 101–107, 1999.

[40] P. H. Mutin, ‘‘Control of the composition and structure of silicon oxycarbide and oxynitride glasses derived from polysiloxane precursors,’’ *Journal of Sol-Gel Science and Technology*, vol. 14, no. 1, pp. 27–38, 1999.

[41] M. Schiavon, S. Redondo, S. Pina, and I. Yoshida, ‘‘Investigation on kinetics of thermal decomposition in polysiloxane networks used as precursors of silicon oxycarbide glasses,’’ *Journal of Non-Crystalline Solids*, vol. 304, no. 1, pp. 92–100, 2002.

[42] E. Radovanovic, M. Gozzi, M. Gonçalves, and I. Yoshida, ‘‘Silicon oxycarbide glasses from silicone networks,’’ *Journal of non-crystalline solids*, vol. 248, no. 1, pp. 37–48, 1999.

[43] K. Eguchi and G. Zank, ‘‘Silicon oxycarbide glasses derived from polymer precursors,’’ *Journal of sol-gel science and technology*, vol. 13, no. 1-3, pp. 945–949, 1998.

[44] Q. Wei, E. Pippel, J. Woltersdorf, M. Scheffler, and P. Greil, ‘‘Interfacial SiC formation in polysiloxane-derived Si–O–C ceramics,’’ *Materials Chemistry and Physics*, vol. 73, no. 2, pp. 281–289, 2002.

[45] R. Haug, M. Weinmann, J. Bill, and F. Aldinger, ‘‘Plastic forming of preceramic polymers,’’ *Journal of the European Ceramic Society*, vol. 19, no. 1, pp. 1–6, 1999.

[46] B. Baufeld, H. Gu, J. Bill, F. Wakai, and F. Aldinger, ‘‘High temperature deformation of precursor-derived amorphous Si–B–C–N ceramics,’’ *Journal of the European Ceramic Society*, vol. 19, no. 16, pp. 2797–2814, 1999.

[47] R. Harshe, C. Balan, and R. Riedel, ‘‘Amorphous Si(Al)OC ceramic from polysiloxanes: bulk ceramic processing, crystallization behavior and applications,’’ *Journal of the European Ceramic Society*, vol. 24, no. 12, pp. 3471–3482, 2004.

[48] G. D. Sorarù, H.-J. Kleebe, R. Ceccato, and L. Pederiva, ‘‘Development of mullite–SiC nanocomposites by pyrolysis of filled polymethylsiloxane gels,’’ *Journal of the European Ceramic Society*, vol. 20, no. 14, pp. 2509–2517, 2000.

[49] H. D. Akkaş, M. L. Öveçoğlu, and M. Tanoğlu, *Development of Si-OC based ceramic matrix composites produced via pyrolysis of a polysiloxane*. Trans Tech Publ, vol. 264, 2004.

[50] M. A. Schiavon, E. Radovanovic, and I. V. P. Yoshida, ‘‘Microstructural characterisation of monolithic ceramic matrix composites from polysiloxane and SiC powder,’’ *Powder Technology*, vol. 123, no. 2, pp. 232–241, 2002.

[51] T. Michalet, M. Parlier, F. Beclin, R. Duclos, and J. Crampon, ‘‘Elaboration of low shrinkage mullite by active filler controlled pyrolysis of siloxanes,’’ *Journal of the European Ceramic Society*, vol. 22, no. 2, pp. 143–152, 2002.

[52] P. Greil, ‘‘Near net shape manufacturing of polymer derived ceramics,’’ *Journal of the European Ceramic Society*, vol. 18, no. 13, pp. 1905–1914, 1998.

[53] P. Greil, ‘‘Near net shape manufacturing of ceramics,’’ *Materials chemistry and physics*, vol. 61, no. 1, pp. 64–68, 1999.

[54] B. Papendorf, K. Nonnenmacher, E. Ionescu, H.-J. Kleebe, and R. Riedel, ‘‘Strong influence of polymer architecture on the microstructural evolution of hafnium-alkoxide-modified silazanes upon ceramization,’’ *Small*, vol. 7, no. 7, pp. 970–978, 2011.

[55] M. A. Schiavon, C. Gervais, F. Babonneau, and G. D. Soraru, ‘‘Crystallization behavior of novel silicon boron oxycarbide glasses,’’ *Journal of the American Ceramic Society*, vol. 87, no. 2, pp. 203–208, 2004.

[56] A. Klonczynski, G. Schneider, R. Riedel, and R. Theissmann, ‘‘Influence of boron on the microstructure of polymer derived SiCO ceramics,’’ *Advanced Engineering Materials*, vol. 6, no. 1-2, pp. 64–68, 2004.

[57] R. Ngoumeni-Yappi, C. Fasel, R. Riedel, V. Ischenko, E. Pippel, J. Woltersdorf, and J. Clade, ‘‘Tuning of the rheological properties and thermal behavior of boron-containing polysiloxanes,’’ *Chemistry of Materials*, vol. 20, no. 11, pp. 3601–3608, 2008.

[58] G. D. Sorarù, R. Pena-Alonso, and H.-J. Kleebe, ‘‘The effect of annealing at 1400°C on the structural evolution of porous C-rich silicon (boron) oxycarbide glass,’’ *Journal of the European Ceramic Society*, vol. 32, no. 8, pp. 1751–1757, 2012.

[59] F. Hönack and R. Riedel, ‘‘Influence of Ti-based fillers on the thermal decomposition and phase development of polysiloxane derived materials,’’ *Advanced Engineering Materials*, vol. 5, no. 3, pp. 122–125, 2003.

[60] P. Greil, ‘‘Active-filler-controlled pyrolysis of preceramic polymers,’’ *Journal of the American Ceramic Society*, vol. 78, no. 4, pp. 835–848, 1995.

[61] S. Dirè, R. Ceccato, and F. Babonneau, ‘‘Structural and microstructural evolution during pyrolysis of hybrid polydimethylsiloxane-titania nanocomposites,’’ *Journal of sol-gel science and technology*, vol. 34, no. 1, pp. 53–62, 2005.

[62] E. Ionescu, C. Linck, C. Fasel, M. Müller, H.-J. Kleebe, and R. Riedel, ‘‘Polymer-derived SiOC/ZrO_2 ceramic nanocomposites with excellent high-temperature stability,’’ *Journal of the American Ceramic Society*, vol. 93, no. 1, pp. 241–250, 2010.

[63] E. Ionescu, B. Papendorf, H.-J. Kleebe, F. Poli, K. Müller, and R. Riedel, ‘‘Polymer-derived silicon oxycarbide/hafnia ceramic nanocomposites. Part I: Phase and microstructure evolution during the ceramization process,’’ *Journal of the American Ceramic Society*, vol. 93, no. 6, pp. 1774–1782, 2010.

[64] R. Chavez, E. Ionescu, C. Fasel, and R. Riedel, ‘‘Silicon-containing polyimide-based polymers with high temperature stability,’’ *Chemistry of Materials*, vol. 22, no. 13, pp. 3823–3825, 2010.

[65] E. Ionescu, H.-J. Kleebe, and R. Riedel, ‘‘Silicon-containing polymer-derived ceramic nanocomposites (PDC-NCs): Preparative approaches and properties,’’ *Chemical Society Reviews*, vol. 41, no. 15, pp. 5032–5052, 2012.

[66] R. Riedel, L. Toma, C. Fasel, and G. Miehe, ‘‘Polymer-derived mullite–SiC based nanocomposites,’’ *Journal of the European Ceramic Society*, vol. 29, no. 14, pp. 3079–3090, 2009.

[67] E. Ionescu, C. Terzioglu, C. Linck, J. Kaspar, A. Navrotsky, and R. Riedel, ‘‘Thermodynamic control of phase composition and crystallization of metal-modified silicon oxycarbides,’’ *Journal of the American Ceramic Society*, vol. 96, no. 6, pp. 1899–1903, 2013.

[68] A. H. Tavakoli, P. Gerstel, J. A. Golczewski, and J. Bill, ‘‘Crystallization kinetics of Si_3N_4 in Si–B–C–N polymer-derived ceramics,’’ *Journal of Materials Research*, vol. 25, no. 11, pp. 2150–2158, 2010.

[69] A. H. Tavakoli, J. A. Golczewski, J. Bill, and A. Navrotsky, ‘‘Effect of boron on the thermodynamic stability of amorphous polymer-derived Si(B)CN ceramics,’’ *Acta Materialia*, vol. 60, no. 11, pp. 4514–4522, 2012.

[70] K. Matsunaga, Y. Iwamoto, C. A. Fisher, and H. Matsubara, ‘‘Molecular dynamics study of atomic structures in amorphous SiCN ceramics.’’ *Journal of the Ceramic Society of Japan*, vol. 107, no. 1251, pp. 1025–1031, 1999.

[71] K. Matsunaga and Y. Iwamoto, ‘‘Molecular dynamics study of atomic structure and diffusion behavior in amorphous silicon nitride containing boron,’’ *J. Am. Ceram. Soc.*, vol. 84, no. 10, pp. 2213–2219, 2001.

[72] A. H. Tavakoli, P. Gerstel, J. A. Golczewski, and J. Bill, ‘‘Kinetic effect of boron on the crystallization of Si_3N_4 in Si–B–C–N polymer-derived ceramics,’’ *Journal of Materials Research*, vol. 26, no. 04, pp. 600–608, 2011.

[73] Y. Iwamoto, K. Kikuta, and S. Hirano, ‘‘Synthesis of poly-titanosilazanes and conversion into Si_3N_4–TiN ceramics.’’ *Journal of the Ceramic Society of Japan*, vol. 108, no. 1256, pp. 350–356, 2000.

[74] Y. Iwamoto, K. Kikuta, and S. Hirano, ‘‘Crystallization and microstructure development of Si_3N_4–Ti(C,N)–Y_2O_3 ceramics derived from chemically modified perhydropolysilazane.’’ *Journal of the Ceramic Society of Japan*, vol. 108, no. 1264, pp. 1072–1078, 2000.

[75] Y. Iwamoto, K. Kikuta, and S. Hirano, ‘‘Si_3N_4–TiN–Y_2O_3 ceramics derived from chemically modified perhydropolysilazane,’’ *Journal of materials research*, vol. 14, no. 11, pp. 4294–4301, 1999.

[76] A. Saha, S. R. Shah, and R. Raj, ‘‘Amorphous silicon carbonitride fibers drawn from alkoxide modified Ceraset^{TM},’’ *Journal of the American Ceramic Society*, vol. 86, no. 8, pp. 1443–1445, 2003.

[77] A. Saha, S. R. Shah, and R. Raj, ‘‘Oxidation behavior of SiCN–ZrO_2 fiber prepared from alkoxide-modified silazane,’’ *Journal of the American Ceramic Society*, vol. 87, no. 8, pp. 1556–1558, 2004.

[78] E. Ionescu and R. Riedel, *Polymer Processing of Ceramics*. John Wiley & Sons, Inc., pp. 235–270, 2012.

[79] T. Prenzel, M. Wilhelm, and K. Rezwan, ‘‘Pyrolyzed polysiloxane membranes with tailorable hydrophobicity, porosity and high specific surface area,’’ *Microporous and Mesoporous Materials*, vol. 169, pp. 160–167, 2013.

[80] R. C. Garvie, ‘‘The occurrence of metastable tetragonal zirconia as a crystallite size effect,’’ *The journal of physical chemistry*, vol. 69, no. 4, pp. 1238–1243, 1965.

[81] A. H. Heuer, N. Claussen, W. Kriven, and M. Rüuhle, ‘‘Stability of tetragonal ZrO_2 particles in ceramic matrices,’’ *Journal of the American Ceramic Society*, vol. 65, no. 12, pp. 642–650, 1982.

[82] F. Babonneau and G. D. Sorarù, ‘‘Synthesis and characterization of Si–Zr–C–O ceramics from polymer precursors,’’ *Journal of the European Ceramic Society*, vol. 8, no. 1, pp. 29–34, 1991.